

December 2010

## ESTIMATING WATER USE THROUGH SATELLITE REMOTE SENSING

---

WRI Technical Completion Report No. 357

Aldo R. Piñón-Villarreal  
Zohrab A. Samani  
A. Salim Bawazir  
Max P. Bleiweiss  
Rhonda Skaggs  
Vien T. Tran



**NEW MEXICO WATER RESOURCES RESEARCH INSTITUTE**  
New Mexico State University  
MSC 3167, Box 30001  
Las Cruces, New Mexico 88003-0001  
Telephone (575) 646-4337 FAX (575) 646-6418  
email: [nmwrri@wri.nmsu.edu](mailto:nmwrri@wri.nmsu.edu)

# **ESTIMATING WATER USE THROUGH SATELLITE REMOTE SENSING**

By

Aldo R. Piñón-Villarreal  
Department of Civil Engineering  
New Mexico State University

Zohrab A. Samani  
Department of Civil Engineering  
New Mexico State University

A. Salim Bawazir  
Department of Civil Engineering  
New Mexico State University

Max P. Bleiweiss  
Department of Entomology, Plant Pathology and Weed Science  
New Mexico State University

Rhonda Skaggs  
Department of Agricultural Economics and Agricultural Business  
New Mexico State University

Vien T. Tran  
Department of Civil Engineering  
New Mexico State University

TECHNICAL COMPLETION REPORT

INDEX NO. 110321

December 2010

New Mexico Water Resources Research Institute

The research on which this report is based was financed in part by the U.S. Department of the Interior, Geological Survey, through the New Mexico Water Resources Research Institute, New Mexico Governor Richardson's WATER INNOVATION FUND (WIF) II, and by the U.S. Department of Agriculture Rio Grande Basin Initiative.

## **DISCLAIMER**

The purpose of the Water Resources Research Institute technical reports is to provide a timely outlet for research results obtained on projects supported in whole or in part by the Institute. Through these reports, we are promoting the free exchange of information and ideas, and hope to stimulate thoughtful discussions and actions that may lead to resolution of water problems. The WRRI, through peer review of draft reports, attempts to substantiate the accuracy of information contained in its reports, but the views expressed are those of the authors and do not necessarily reflect those of the WRRI or its reviewers. Contents of this publication do not necessarily reflect the views and policies of the Department of the Interior, nor does the mention of trade names or commercial products constitute their endorsement by the United States government.

## **ACKNOWLEDGEMENT**

This report was submitted as a partial fulfillment for the Master of Science degree in civil engineering at New Mexico State University, by Aldo R. Piñón-Villarreal. Special thanks to Ms. Leeann S. De Mouche for administrative support, to Ms. Julie Moore for editorial assistance, to Stahmann Farms, and to Mr. Marshall Clayshulte for orchard access and cooperation in this research. Thanks to the following students for their assistance in the field for maintaining instrumentation and data collection: Jimmy Moreno, Atzuko Reveles, Eric Lopez, Brad Kirksey, David Fabre, Jose Solis, Kate Adams, Marco Gamboa, and Ernesto Santillano. We extend our gratitude to anonymous reviewers whose comments and suggestions greatly improved the quality of this report.

## ABSTRACT

The Mesilla Valley, New Mexico is a major producer of pecans in the southwestern United States. Irrigation for pecans constitutes the largest consumer of surface water from the Rio Grande. In order to develop an effective water budget for the region, improved estimates of regional evapotranspiration (ET) are needed. The Regional ET Estimation Model (REEM) using satellite imagery from ASTER and Landsat-7 sensors, and ground-measured meteorological data were used to determine ET of pecan orchards in the Valley for the year 2002. Geographic information systems (GIS) vector files, each representing a single pecan orchard, were superimposed over the REEM output maps to obtain estimates of orchard area and ET. The total areas for the orchards greater than 4 ha (10 acres) and less than 4 ha (10 acres) were determined as 7,969 ha (19,691 acres) and 1,851 ha (4,573 acres), respectively. The weighted average annual ET of the larger orchards was determined as 991 mm using ASTER data and 1,018 mm using Landsat-7 data compared to 800 mm and 852 mm for the smaller orchards using ASTER and Landsat-7 data respectively. The spatial and temporal variability in ET was analyzed among 280 sampled orchards greater than 4 ha (10 acres). Standard deviation of ET using ASTER and Landsat-7 data ranged from 3.45 to 28.40 and 1.70 to 27.13 mm/month in December and in May, respectively.

A method to estimate ET in pecan orchards was developed by relating the fractional cover (fc), the normalized vegetation index (NDVI) and REEM annual ET for 280 pecan orchards. Orchard fc was estimated using supervised classification of aerial photography (color infrared-Digital Ortho-photo Quarter-Quadrangles or CIR-DOQQs). This method compared well with field measurements of fc carried out in thirteen pecan orchards from the Valley (mean percentage error = 14%). Linear regression of the fc determined by supervised classification and the NDVI resulted in a coefficient of determination ( $R^2$ ) of 0.71 ( $n = 170$ ). This relationship was then used to relate fc to the REEM annual ET via NDVI for 280 pecan orchards for the Mesilla Valley.

## TABLE OF CONTENTS

DISCLAIMER .....	ii
ACKNOWLEDGEMENT .....	iii
ABSTRACT .....	iv
LIST OF TABLES .....	vii
LIST OF FIGURES .....	viii
1. INTRODUCTION.....	1
1.1. Purpose and Objectives of the Study.....	3
1.2. Scope and Limitations .....	4
2. BACKGROUND.....	5
2.1. Pecan Production in New Mexico .....	5
2.2. Evapotranspiration of Pecan Reported in Literature .....	7
2.3. Using Remote Sensing to Determine Agronomic Parameters .....	9
2.4. Remote Sensing Methods for Estimating ET .....	12
3. DESCRIPTION OF THE STUDY AREA .....	13
3.1. Location and Physiography .....	13
3.2. Hydrogeology .....	15
3.3. Climate .....	15
3.4. Spatial Extent of the Study .....	16
4. REGIONAL EVAPOTRANSPIRATION ESTIMATION MODEL (REEM).....	18
4.1. Satellite Data .....	18
4.2. Calculation of Regional ET .....	19
5. METHODOLOGY .....	21
5.1. Estimation of Pecan ET and Acreage at the Orchard Level.....	21
5.2. Estimation of Fractional Cover Using Aerial Photography and Remote Sensing.....	25
5.2.1. Estimation of fractional cover with supervised classification of CIR-DOQQs.....	25

5.2.2.	Calculation of vegetation indices .....	28
5.2.3.	Field measurements of fractional cover .....	30
5.3.	Development of a Method to Estimate ET from Fractional Cover .....	32
6.	RESULTS AND DISCUSSION .....	34
6.1.	Distribution of Acreage among the Pecan Orchards .....	34
6.2.	REEM Estimated Pecan ET .....	36
6.3.	Comparison of Estimated Pecan ET and ET Published in Literature .....	40
6.4.	Estimation of Fractional Cover in the Pecan Orchards .....	41
6.5.	Relationship between Fractional Cover and Vegetation Indices.....	44
6.6.	Predicting ET as a Function of Midseason NDVI and Fractional Cover .....	48
7.	SUMMARY AND CONCLUSIONS.....	53
7.1.	Summary .....	53
7.2.	Conclusions .....	53
7.3.	Recommendations .....	54
	REFERENCES .....	56

## LIST OF TABLES

Table	Page
1. Comparison of Various Pecan ET Measurements from Published Literature.....	8
2. Acquisition Dates for the ASTER and Landsat-7 Images .....	18
3. Arrangement of Spectral Bands in True-color and Color-infrared DOQQs .....	26
4. Differences in Acreage and Number of Pecan Orchards Using Three Different Maps .....	35
5. Weighted Annual Average or Mean ET for the Pecan Orchard Categories Using the ASTER and Landsat-7 Data Sets .....	37
6. Statistics for Mean Monthly ET for 280 Pecan Orchards Using ASTER and Landsat-7 Data During 2002 .....	39
7. Comparison of Seasonal ET Estimated with Landsat-7 and ASTER Data Compared with Those Published in Literature.....	41
8. Measured Field Parameters of Thirteen Pecan Orchards.....	43
9. Measured Versus Estimated $f_c$ in Thirteen Pecan Orchards.....	44
10. Linear Regression Statistics for Estimating $f_c$ from NDVI, SAVI and $\theta_{SAVI}$ .....	45



## LIST OF FIGURES

Figure	Page
1. Area Planted with Pecans in Doña Ana County, New Mexico from 1974-2002 .....	6
2. Pecan Production in Doña Ana County, New Mexico from 1959-2006 .....	6
3. Map of the Study Area.....	14
4. Spatial Extent of the Study (Mesilla Valley) .....	17
5. Delineated Pecan Orchards (as White Polygons) in the Mesilla Valley, New Mexico .....	23
6. Digitized Vectors of the Pecan Orchards (White Solid Lines) Overlaid in a REEM Annual ET Map by Using the Region of Interest (ROI) Tool in ENVI® .....	24
7. Example of Supervised Classification of a CIR-DOQQ for Estimating Fractional Cover (fc) .....	27
8. Designation and Spatial Location of the Orchards Measured for fc in a Pecan Farm.....	31
9. Sketch of the Method Used to Measure the Projected Area of Tree Canopy and fc .....	33
10. Distribution of Area for 1,779 Pecan Orchards in the Mesilla Valley as Projected in the DOQQ Mosaic.....	36
11. Histogram of Annual ET for All the Pecan Orchards (n = 1,779 and 1,778) Using ASTER and Landsat-7 Data During 2002 .....	37
12. Relationship between Orchard Size and Annual ET for 1,779 Pecan Orchards in the Mesilla Valley Using 2002Landsat-7 Data .....	40
13. Histogram of fc Values Estimated with the Supervised Classification Method for 170 Pecan Orchards During 2005.....	43

14.	Linear Relationship between $f_c$ and NDVI for 170 Pecan Orchards in the Mesilla Valley from an ASTER Image Acquired on September 28, 2005 .....	46
15.	Linear Relation between $NDVI_{Landsat}$ and $NDVI_{ASTER}$ Values Obtained for 280 Pecan Orchards in the Mesilla Valley from an Observation Made on May 15, 2002.....	47
16.	Relationship Between $f_c$ and ASTER NDVI Converted to Landsat-7 NDVI Using Equation 7 for 170 Pecan Orchards in the Mesilla Valley on September 28, 2005.....	48
17.	Linear Relation between Midseason NDVI from a Landsat-7 Scene from June 16, 2002 and REEM Annual ET for 280 Pecan Orchards in the Mesilla Valley.....	50
18.	Linear Relation between Midseason $f_c$ Calculated from an NDVI Image for June 16, 2002 and REEM Annual ET for 280 Pecan Orchards in the Mesilla Valley .....	51

## 1. INTRODUCTION

The Mesilla Valley, New Mexico is a unique agricultural region of the southwestern United States. Most of the water used for agriculture in the Valley comes from the Rio Grande, which is the main source of surface and groundwater in the region. The water from the river is stored in the Elephant Butte Reservoir located 121 km north of the Mesilla Valley where the U.S. Bureau of Reclamation controls its release. For more than a decade, the water stored in the Elephant Butte Reservoir has continued to decline due to drought in the region. In addition, population in the three largest cities that are within or near the Mesilla Valley area (Las Cruces, New Mexico, El Paso, Texas, and Ciudad Juárez, México) has increased between 15 and 50% from 1990 to 2000, and is expected to grow between 60 and 150% by the year 2030 (King and Maitland, 2003). To ensure availability of water for future needs, it will be necessary to transfer part of the available water from agriculture to industrial and municipal uses (Skaggs and Samani, 2005). Before that can be done, water use from current irrigation practices needs to be quantified to determine the impact that the transfer of water supplies would have on the general hydrology and water availability of the region.

Among current agricultural water use, irrigation for pecans constitutes the largest consumer of the surface water from the Rio Grande. Pecan is an important crop that contributes to the local economy of the Mesilla Valley. According to *2002 Census of Agriculture*, in Doña Ana County, New Mexico pecans constituted 31% of the total irrigated land (82,780 acres or 33,500 ha), followed by alfalfa (21%) and cotton (18%) during 2001 (U.S. National Agricultural Statistics or NASS, 2007).

Pecans also demand large amounts of water when compared to other crops in the region (Reveles, 2005; Sammis et al., 2004; Miyamoto, 1983). Therefore, accurate quantification of its water use or evapotranspiration (ET) in the Valley is critical for conducting an effective water budget for the region.

The ET in pecans varies due to tree varieties, planting densities, soil types, and agricultural practices (irrigation, fertilization, pruning, etc.) across the Valley. A cost-effective approach for determining ET on spatial and temporal scale at the regional level is to use remote sensing technology. Recently, researchers at New Mexico State University (NMSU) have developed a surface energy balance (SEB) model known as Regional ET Estimation Model (REEM) that allows the estimation of crop ET over large areas. The REEM uses satellite imagery, ground-level ET measurements and climatic data for the estimation of regional ET.

Studies carried out by Samani and others (2009) showed a good agreement between ET estimated by REEM and ground measurements using eddy covariance (EC) technique in riparian and agricultural ecosystems. In this study, monthly and annual ET of pecan orchards were analyzed using ET maps generated with REEM using data from two different satellite instruments. Satellite data used were from the Advanced Spacernone Thermal Emission and Reflection (ASTER) and the Landsat-7 Enhanced Thematic Mapper Plus (ETM+) radiometers. Pecan orchards in the Mesilla Valley were delineated using geographic information system (GIS) techniques and high resolution aerial photography.

In addition, a methodology to estimate ET of pecan orchards was developed based on both the vegetation fractional cover (fc) and the normalized difference

vegetation index (NDVI). Previous studies have demonstrated that  $f_c$  is linearly related to plant transpiration (Trout and Johnson, 2007; Goodwin et al., 2004; Johnson et al., 2002, 2000). In this study, it was hypothesized that ET is directly related to the  $f_c$  on an orchard basis and that the seasonal ET in pecans present a high variability among the orchards in the Valley due to different agricultural practices and environmental factors.

### 1.1. Purpose and Objectives of the Study

The purpose of this study was to perform a regional evaluation of pecan ET on an orchard basis in the Mesilla Valley, New Mexico and to relate pecan ET to the fractional cover ( $f_c$ ), which could be measured easily in the field. The specific objectives were:

1. Use GIS vector files (each representing a single orchard) along with remotely sensed data and aerial photography to determine the extent and distribution of pecan orchard areas in the Valley;
2. Use the pecan vectors (orchard) and REEM with ASTER and Landsat-7 data to analyze the spatial variation of ET among the orchards in the Valley;
3. Estimate  $f_c$  in the pecan orchards by applying a method that uses digital analysis of aerial photography;
4. Relate  $f_c$  to vegetation indices (VIs) calculated from remotely sensed data for the pecan orchards to establish models of the relationships;
5. Determine the relationship between  $f_c$  and ET via VIs and develop a methodology to predict annual ET of pecan orchards.

## 1.2. Scope and Limitations

The scope of this study was a regional evaluation of pecan water use in the Mesilla Valley using the REEM model and GIS data. The ET rates obtained through the model were compared with measured values only in one location, thus the accuracy of the results obtained in the remaining orchards could not be verified on a field basis but only on a regional scale using volume-balance analysis. The information on water application and frequency of irrigation in most fields was limited, impeding the evaluation of irrigation and management practices. In addition, there was limited information on farm yield and crop stress caused by factors such as soil types, nutrient deficiencies, pests and diseases, which made it difficult to explain the causes of variability in ET among pecan orchards.

## 2. BACKGROUND

### 2.1. Pecan Production in New Mexico

Pecan [*Carya illinoensis* (Wangenh.) C. Koch] is a deciduous tree indigenous to the Mississippi river and tributaries. In the Southwest, pecans have been established in New Mexico, Arizona, and California (Manaster, 1994). The adaptability of pecans to grow outside their native range can be attributed to freeze tolerance and reduction of fruit production under severe winters and short growing seasons (Sparks, 2005). In New Mexico, the combination of good irrigation practices and plenty of sunshine has overcome the disadvantage of the native short growing season, and has enhanced the commercial production of pecans (Herrera, 2005).

Total production in the United States increased from 25 million pounds in 1924 (Herrera, 2000) to 262 million pounds in 2003. In 1999, the production in the U.S. was more than 400 million pounds (NASS, 2004). New Mexico was ranked third after Georgia and Texas in pecan production totaling 55 million pounds with earnings of 70.4 million dollars in 2003 (NASS, 2004). Pecan production has increased considerably in the Mesilla Valley in the last 40 years. This has positioned Doña Ana County as one of the leading counties in the production of pecan nationwide (Herrera, 2000). The land planted with pecans in Doña Ana County increased from 3,360 ha (8,300 acres) in 1974 (U.S. Bureau of the Census, 1977) to 10,526 ha (26,000 acres) in 2002 (NASS, 2007). See Figure 1. In 2002, 26 million pounds of pecans (in shell) were produced in the County, which accounted for the 72% of all the production in New Mexico (NMAAS, 2004). Figure 2 shows the pecan production in Doña Ana County from 1959 to 2006.

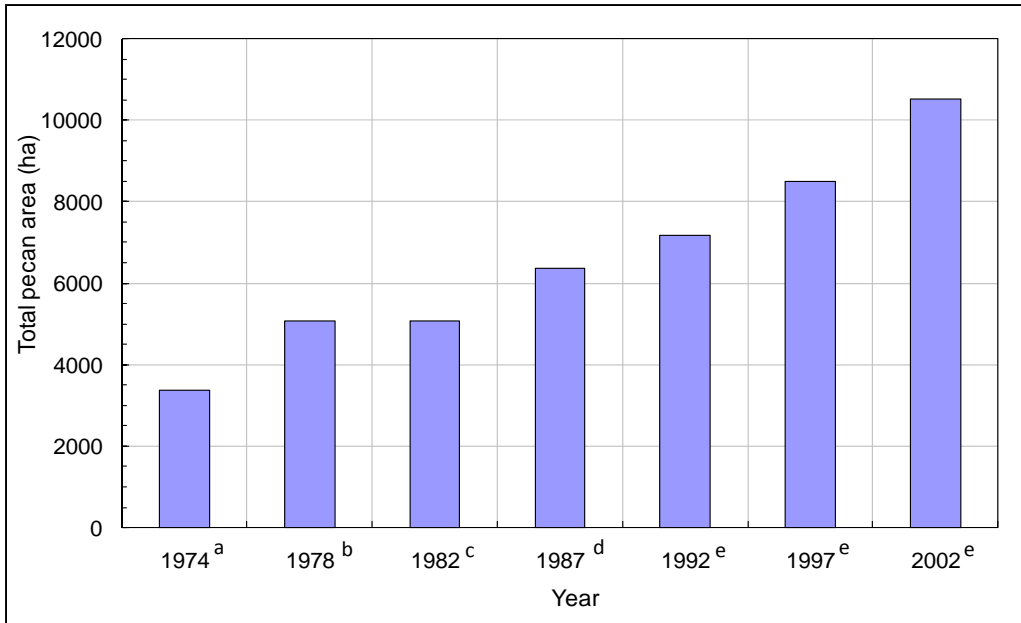


Figure 1. Area Planted with Pecans in Doña Ana County, New Mexico from 1974-2002 (Source: U.S. Bureau of the Census for a,b,c,d; National Agricultural Statistics Service, NASS, for e)

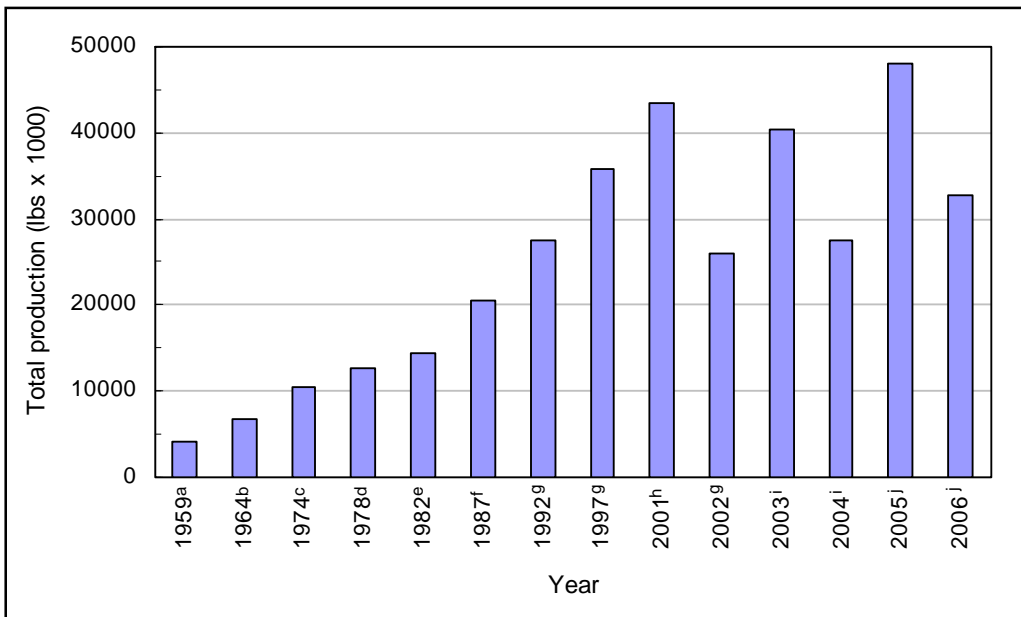


Figure 2. Pecan Production in Doña Ana County, New Mexico from 1959-2006 (Source: U.S. Bureau of the Census for a,b,c,d,e,f; National Agricultural Statistics Service, NASS, for g; New Mexico Agricultural Statistics, NMAS, for h,i,j)



## 2.2. Evapotranspiration of Pecan Reported in Literature

Different methods have been used by researchers to estimate or measure ET of pecan trees. Miyamoto (1983) evaluated water use (or ET) of surface-irrigated pecan trees in seven commercial orchards in the Lower Rio Grande Valley (El Paso, TX and Las Cruces, NM Valleys). The trees studied ranged in age from 8 to 35 years old and had trunk diameters ranging from 13 to 53 cm. He reported pecan water use for the growing season (April through October) ranging from 368 to 1,307 mm depending on tree size and planting density; high ET rates between 1,000 to 1,300 mm were determined for full-grown trees.

Steinberg and others (1990) measured trunk and branch sap flow to determine canopy transpiration in order to quantify water fluxes through young pecan trees in Stephenville, Texas. Two five-year old pecan trees ('Wichita' variety) were planted in two cylindrical lysimeters of 2.44 m in diameter and 1.52 m in depth; tree transpiration was determined as the difference in weight after irrigation events. The trees had a height of 3.9 m, and trunk diameter of 7.9 cm. An average tree ET of 5.66 mm/day was measured over a 12 day period (August 18 to August 30, 1988) using the water budget method.

Frías-Ramírez (2002) evaluated ET and light interception at branch and tree levels in a commercial pecan orchard located 8 km southwest of Las Cruces, New Mexico during 1996 and 1997. The orchard had 'Western Schley' trees. The trees were about 28 years old with canopy height of 15 m. The purpose of the study was to measure ET with the soil water budget method and compare it with an assimilation-transpiration model (via light interception) and ET calculated using Miyamoto (1983)

crop coefficient. From the study, using the soil water budget method, Frías-Ramírez (2002) reported a cumulative ET of 1,120 mm during 1996 and 1,020 mm in 1997.

Reveles (2005) measured ET during 2004 and part of 2005 using the eddy covariance technique in a commercial pecan orchard about 13 km south of Las Cruces. The orchard was planted with ‘Western Schley’ trees. The trees were 40 and 65 years old with trunk diameters of 38 and 50 cm, respectively, and average height of 16 m. He reported an ET value of 1,255 mm in 2004 (April to November – growing season). The total annual ET in 2004 was 1,389 mm and 1,221 mm for 268 days in 2005 (January 1 to September 25). Table 1 summarizes ET of pecan from studies reported in literature.

Table 1. Comparison of Various Pecan ET Measurements from Published Literature

Reference	Location	Method	Date measured	ET	Water table
Reveles (2005)	Mesilla Valley, NM	EB-EC <sup>a</sup>	Jan-Dec 2004 Jan-Sep 25, 2005	1.39 m/yr 1.22 m/yr	2.2 m <sup>b</sup> 2.1m
Sammis and others (2004)	Mesilla Valley, NM	EB-EC	Apr-Nov 20, 2001 Apr-Nov 6, 2002	1.26 m/sea <sup>c</sup> 1.17 m/sea	– <sup>d</sup>
Frías-Ramírez (2002)	Mesilla Valley, NM	Water balance	Jan-Dec 1996 Jan-Dec 1997	1.12 m/yr 1.02 m/yr	– <sup>d</sup>
Steinberg and others (1990)	Stephenville, TX	Heat balance lysimeters	Aug 18-Aug 30, 1988	5.66 mm/day	– <sup>d</sup>
Miyamoto (1983)	El Paso, TX Mesilla, NM	Soil water depletion <sup>c</sup>	Apr-Oct 15, Long term	0.36-1.31 m/yr	> 3.0 m

<sup>a</sup>Energy balance-eddy covariance

<sup>b</sup>Water table during growing seasons (Apr-Nov, 2004 and Apr-Sep 2005)

<sup>c</sup>Units are in meters for the growing season

<sup>d</sup>Data not reported

<sup>e</sup>Referred to as *soil water balance* in this study

### 2.3. Using Remote Sensing to Determine Agronomic Parameters

The use of remotely sensed energy reflected or emitted from the earth's surface in the visible (0.4-0.7  $\mu\text{m}$ ), near-infrared (0.7-1.1  $\mu\text{m}$ ) and thermal infrared (10-13.4  $\mu\text{m}$ ) regions of the electromagnetic spectrum has found many applications. Remote sensing has been used widely in the field of irrigated agriculture to determine important agronomic parameters such as fractional cover ( $f_c$ ), leaf area index (LAI), crop type, crop yield, and crop stress (Bastiaanssen, 1998). Fractional cover ( $f_c$ ) was defined by Bastiaanssen (1998) as "the portion of land covered by at least one layer of plant canopies at nadir orientation." The importance of  $f_c$  is that it determines the amount of solar radiation intercepted by the plant canopy (available for photosynthesis) and regulates soil and canopy fluxes. Fractional cover can be determined by combinations of visible and near-infrared (NIR) spectral measurements or vegetation indices (VIs) (Bastiaanssen, 1998). In addition, several investigators have demonstrated that  $f_c$  is related linearly to plant transpiration (Trout and Johnson, 2007; Goodwin et al., 2004; Johnson et al., 2002, 2000; Choudhury et al., 1994).

The leaf area index (LAI), defined as the total area of leaves per unit area of land at nadir orientation, is an important vegetation parameter used in many studies to estimate canopy density, biomass and crop yield, and it is used in equations concerning canopy resistance and heat fluxes (Bastiaanssen, 1998). The LAI can also be related to various VIs (Choudhury et al., 1994).

The crop type can be determined by applying thematic land classification algorithms to spectral measurements done in individual bands (Bastiaanssen, 1998).

Vegetation indices and crop models are used for the determination of crop yield (Liang et al., 2004). Other parameters such as relative evapotranspiration (ratio of actual ET to potential ET) could be used as an indicator for crop stress (Roerink et al., 1997).

The determination of these and other crop parameters has been accomplished largely by the utilization of VIs computed from remotely sensed data. Vegetation indices are spectral indices that detect the presence of chlorophyll (the green component of most plants) in the red (0.62-0.70  $\mu\text{m}$ ) and near-infrared (NIR) (0.7-1.1  $\mu\text{m}$ ) regions of the electromagnetic spectrum. For decades the use of VIs has constituted a method for extracting vegetation biophysical parameters from radiometric observations (Jiang et al., 2006).

The normalized difference vegetation index (NDVI) defined as the difference between the NIR and red reflectance divided by their sum is one of the most widely used VIs in agricultural, land cover, and climatic studies (Jiang et al., 2006). The NDVI is calculated with the expression (Tucker, 1979):

$$\text{NDVI} = \frac{\rho_{\text{NIR}} - \rho_{\text{R}}}{\rho_{\text{NIR}} + \rho_{\text{R}}} \quad (1)$$

where,  $\rho_{\text{NIR}}$  is reflectance in the near-infrared band and  $\rho_{\text{R}}$  is reflectance in the red band.

A variety of indices have been developed to produce improved correlations to biophysical parameters such as  $f_c$  and LAI (Jiang et al., 2006; Bastiaanssen, 1998;

Huete et al., 1985). The soil-adjusted vegetation index (SAVI) was developed to take into account the influences of soil background effects (Huete, 1988). This index introduced an adjustment factor,  $L$ , to shift the origin of the NIR/red wavelength space towards a convergence point for different isolines (lines of constant vegetation amount) when the NIR and red reflectances are plotted together. The adjustment factor is inversely proportional to the vegetation amount or LAI and can be chosen based on prior knowledge about the vegetation. In the absence of field data, Huete (1988) recommended the use of a constant “ $L$ ” value of 0.5. The soil-adjusted vegetation index (SAVI) is calculated with the expression:

$$SAVI = \frac{\rho_{NIR} - \rho_R}{\rho_{NIR} + \rho_R + L} (1 + L) \quad (2)$$

More recently, an angle-based VI was developed to avoid the NDVI saturation problem at high vegetation densities (Carlson and Ripley, 1997) and the noise created by different soil backgrounds (Huete et al., 1985). This index is called theta-soil adjusted vegetation index ( $\theta_{SAVI}$ ), and was modified from SAVI using trigonometric analysis (Jiang et al., 2006). This index detects vegetation amounts by the angle between the theoretical soil line and a simulated vegetation isoline, and is calculated after Jiang and others (2006) as:

$$\theta_{SAVI} = 2 \arctan \left( \frac{\rho_{NIR} - \rho_R}{\rho_{NIR} + \rho_R + L} \right) = \frac{SAVI}{1.5}. \quad (3)$$

#### 2.4. Remote Sensing Methods for Estimating ET

The methods that use remote sensing technology to estimate ET have evolved substantially over the last 30 years. Many algorithms that are based on the energy balance approach have been created or refined in the last decade. This is due in part to the increase in availability of satellite observations and a significant reduction in the cost of satellite scenes (Allen et al., 2008).

Evapotranspiration cannot be measured directly from satellite observations; most remote sensing models that estimate ET are based on the energy budget principle in which the latent heat (LE) is calculated indirectly as a residual. Several regional ET estimation models have been developed and are documented in literature (Samani et al., 2009; Allen et al., 2005a; Bastiaanssen et al., 2005; Bastiaanssen et al., 1998a,b; Bastiaanssen, 1995). In this study, the Regional ET Estimation Model (REEM) was used to determine regional ET in the Mesilla Valley, southern New Mexico. The algorithm of REEM is detailed in Samani and others (2009).

### 3. DESCRIPTION OF THE STUDY AREA

#### 3.1. Location and Physiography

The study area is located in the Mesilla Valley, southwestern part of the Doña Ana County, New Mexico. The Mesilla Valley is in the floodplain of the lower Rio Grande that starts at the narrows of Selden Canyon just north of Leasburg, New Mexico from where it follows the course of the Rio Grande in a southeastern direction until it reaches the narrows formed by the Franklin and Sierra de Juárez Mountains at El Paso, Texas (New Mexico Office of the State Engineer (NM-OSE), 2000). The Valley is 72.4 km long, is very flat with gentle slopes, varying in width from less than 1.6 km to around 8 km (Bulloch and Neher, 1980). It is bounded on the north by the Robledo and Doña Ana Mountains, on the west by the West Mesa and the Potrillo Mountains, on the south by the Franklin and Sierra de Juárez Mountains, and on the east by the Organ and Franklin Mountains (NM-OSE, 2000). The elevation in the area ranges from 1,137 meters in the Valley to 1,524 meters above sea level (ASL) in the upland plains (Figure 3).

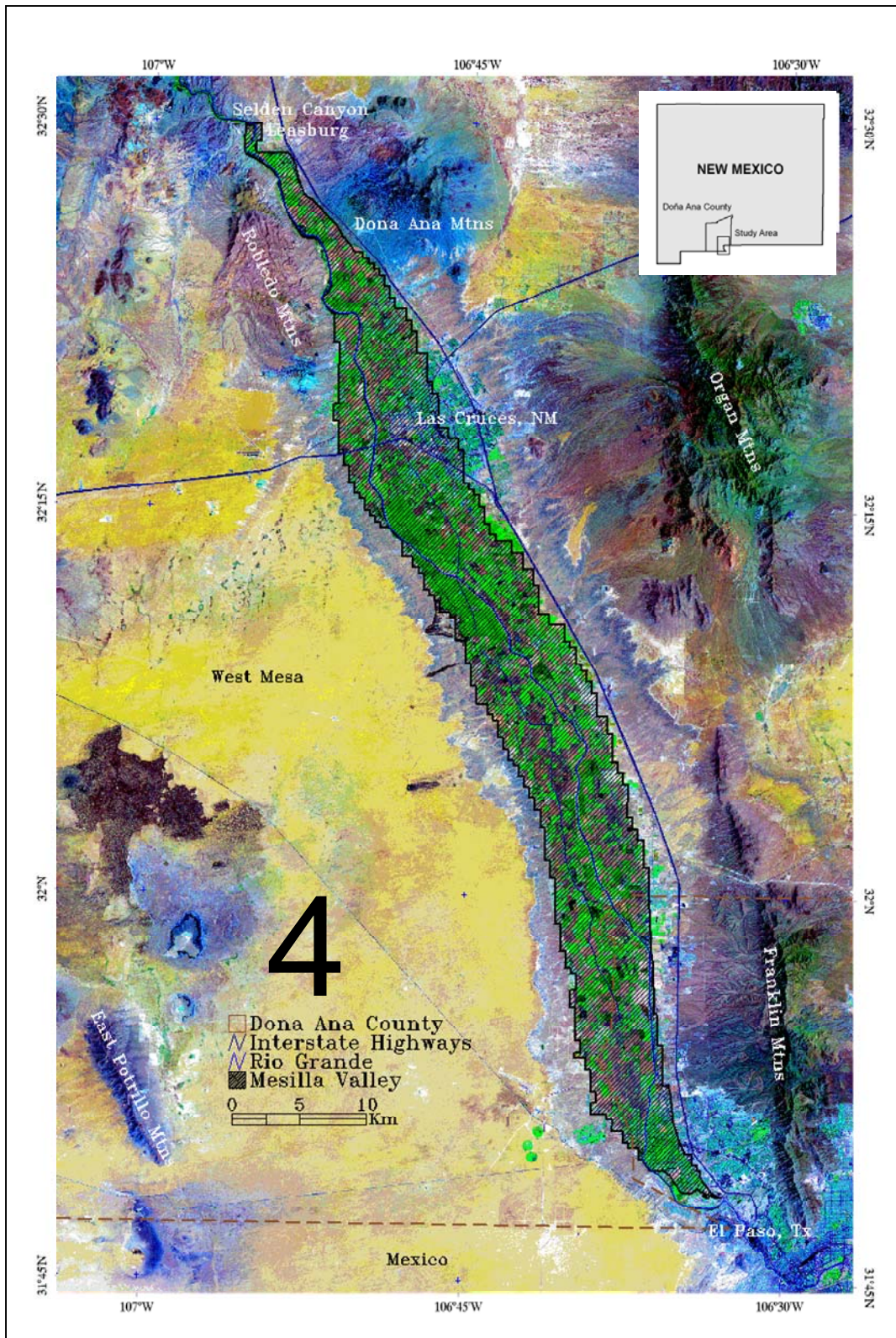


Figure 3. Map of the Study Area. The Image is a False Color Landsat-7 Scene Showing the Mesilla Valley, Year 2000



### 3.2. Hydrogeology

The geological setting of the Mesilla Valley was described by Weeden and Maddock (1999) as the rift of the Rio Grande with chains of mountains aligned in the northwest-southeast direction. The flood plain of the Rio Grande Basin is filled with alluvial deposits (Weeden and Maddock, 1999). The aquifer systems of the Valley include thin quaternary fluvial deposits (valley-fill aquifer system) and thick sedimentary fill of intermontane basins (basin-fill aquifer system) composed of the Cenozoic Santa Fe group (Hawley and Kennedy, 2004). These deposits constitute the main water bearing strata referred to as the Mesilla Basin, the major source of the groundwater supply to the region.

### 3.3. Climate

The study area has a semi-arid climate characterized by low and variable total precipitation, large diurnal and moderate temperature ranges, low relative humidity, and ample sunshine (Malm, 2003). The mean total annual precipitation of the area based on 109 years (1892-2000) of historical record as reported by Malm (2003) is 222 mm. More than half of total precipitation occurs during the monsoonal months of July through September. The monsoon season, in which nearly three-fourths of total annual precipitation occurs, is May through October. November through May constitutes the dry season with an average monthly precipitation of 13 mm or less (Malm, 2003).

Based on 109 years of historical weather records (1892-2000) for Las Cruces, the nearest large city to the study area, the average maximum daily temperatures

during the year is 24.83 °C and average minimum daily temperature during the year is 6.78 °C (Malm, 2003). The mean annual relative humidity ranges from 26% to 52% (Table 7 in Malm, 2003); low relative humidity values often occur in the months of April through June while high values occur during the midwinter and midsummer. These elevated relative humidity values are related to rainfall patterns. The winds in the study region are usually light with mean annual wind speed of 2.68 m/s (Malm, 2003). In this region, wind flows generally from the southwest direction.

#### 3.4. Spatial Extent of the Study

The spatial extent of the study was confined to the area of the Mesilla Valley as projected in one of the Landsat-7 images. The satellite image shown in Figure 3 was spatially registered to a dataset of GIS vector files representing pecan orchards from Doña Ana County. The remaining ASTER and Landsat-7 satellite data were registered and subsetting to conform to this image. A total area of 46,359 ha (114,556 acres) was delineated for the Mesilla Valley (Figure 4). The Universal Transverse Mercator (UTM) coordinate system referenced to the World Geodetic System of 1984 (WGS-84) datum was used to define the bounding coordinates of the study area. The coordinates of the upper left corner of the study area were 318,634.59, 3,597,298.25 meters (106° 55' 49.58" West and 32 ° 29' 53.50" North), and the coordinates of the lower right corner were 353,613.66, 3,519,952.39 meters (106° 32' 48.24" W and 31° 48' 21.17" N). The pecan orchards considered in this study were located within the Mesilla Valley from Leasburg Dam, New Mexico where the water is diverted for irrigation, to the border of New Mexico-Texas at

Courchesne Gaging Station where the outflow from the Valley in the Rio Grande is measured.

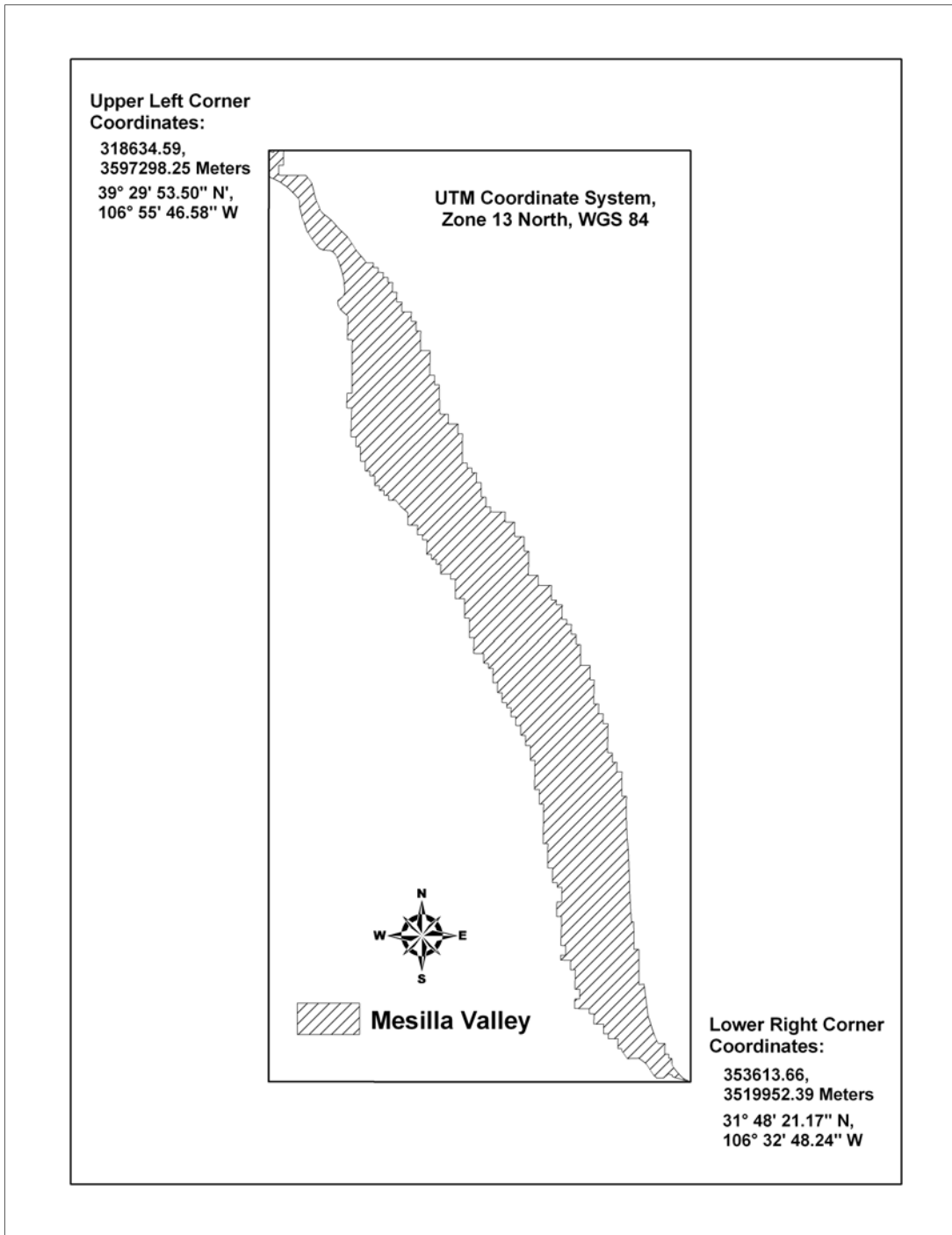


Figure 4. Spatial Extent of the Study (Mesilla Valley)

#### 4. REGIONAL EVAPOTRANSPIRATION ESTIMATION MODEL (REEM)

##### 4.1. Satellite Data

The satellite data used in this study consisted of satellite imagery acquired by the Advanced Spaceborne Thermal Emission and Reflection Radiometer (ASTER) and the Landsat-7 Enhanced Thematic Mapper Plus (ETM+) radiometer. The data consisted of spectral observations on different wavelengths for the year 2002. The year 2002 was chosen to be analyzed since it was a full allocation year in terms of water delivery to the farmers with a total allotment of 9,014.4 m<sup>3</sup>/ha or 3 acre-ft/acre. The images were obtained from the Land Processes Distributed Active Archive Center (LPDAAC, <http://lpdaac.usgs.gov/main.asp>) which is part of the National Aeronautics and Space Administration-Earth Observing System Data and Information System (NASA-EOSDIS). Acquisition dates for the ASTER and Landsat-7 ETM+ images used in this study are listed in Table 2.

Table 2. Acquisition Dates for the ASTER and Landsat-7 Images

ASTER	Landsat-7 ETM+	
Jan 23,2002	Jan 23, 2002	Jul 02, 2002
Feb 08, 2002	Feb 08, 2002	Sep 04, 2002
May 15, 2002	Feb 24, 2002	Sep 20, 2002
Aug 19, 2002	Mar 12, 2002	Oct 06, 2002
Nov 07, 2002	May 15, 2002	Dec 09, 2002
Nov 23, 2002	May 31, 2002	
Dec 09, 2002	Jun 16, 2002	

The ASTER sensor makes multispectral observations over a large spectral range from the visible to the thermal infrared regions with high spatial, spectral, and radiometric resolution (Abrams et al., 2002). The spatial resolution varies with the

wavelength (Visible Near Infrared, VNIR = 15 m, ShortWave Infrared, SWIR = 30 m, and Thermal Infrared, TIR = 90 m spatial resolution). Each scene covers approximately 60 by 60 km, and the ASTER products (usually individual bands) are processed and distributed in an “on demand” basis (Abrams et al., 2002).

The Landsat-7 satellite uses the Enhanced Thematic Mapper plus (ETM+) instrument to map the earth’s surface. The ETM+ is a nadir viewing, eight-band multispectral scanning radiometer with high resolution (Visible Near Infrared, VNIR = 30 m, Shortwave Infrared, SWIR = 30 m, and Thermal Infrared, TIR = 60 m of spatial resolution). A typical scene of the Landsat imager covers 180 by 60 km (Landsat Project Science Office (LPSO), 2007). The orbit of both Terra (ASTER) and Landsat-7 satellites are circular, sun-synchronous, and near polar with a 16-day repeated cycle (Abrams et al., 2002; LPSO, 2007). Further details of ASTER data and the atmospheric and geometric corrections of the imagery were described by Samani and others (2007a) and those for Landsat-7 by Samani and others (2009).

#### 4.2. Calculation of Regional ET

The Regional Evapotranspiration Estimation Model (REEM) (Samani et al., 2009, 2007a, 2007b) was used to calculate daily ET of pecan in the study area. The REEM uses satellite, weather data and localized ET measurements to estimate regional ET. The algorithm used by the REEM model was described in detail by Samani and others (2009). The REEM was run in the interactive data language (IDL®) software platform of the software package *Environment for Visualizing Images* (ENVI®) developed by Research Systems Inc. (RSI, Boulder, Colorado). The

algorithm was run using data input from 19 observations from two satellites (ASTER and Landsat-7) as described in Table 2 and weather data from Chamberino Weather Station (CWS) located in the Valley (latitude 32° 3' 43.97" N and longitude 106° 40' 43.36" W). The weather station data were used to calculate the daily American Society of Civil Engineers (ASCE) standardized reference evapotranspiration (ET<sub>sz</sub>) following Allen and others (2005b). Evapotranspiration maps resulting from the REEM algorithm were re-sampled to have a pixel size of 15 m using ASTER data, and to a pixel size of 30 m using Landsat-7 data. The outputs of REEM were regional ET maps for each spectral observation representing spatial and temporal values of ET in every pixel. The details of REEM ET estimates, comparison to measured ET using eddy covariance method, and daily ET estimates for those days when no useable satellite data was available were presented in Samani and others (2009).

## 5. METHODOLOGY

### 5.1. Estimation of Pecan ET and Acreage at the Orchard Level

In order to obtain ET estimates for individual fields, first the pecan orchards in the Mesilla Valley were delineated. Geographic information system (GIS) vector files were used to represent the orchards in the remote sensing model. A database of vector files were first obtained from the Doña Ana County Office located in Las Cruces, New Mexico. This database of vector files was based on tax records and divided the orchards in two groups: orchards greater than 4 ha (10 acres) and smaller than this size. However, this database of vector files did not include all the orchards in the Valley. Therefore, the 2005 U.S. Geological Survey (USGS) Digital Ortho-photo Quarter-Quadrangles (DOQQs) released by the New Mexico Geospatial Data Acquisition Coordination Committee (GDACC) and downloaded from the New Mexico Resource Geographic Information System Program website (NM-RGIS, <http://rgis.unm.edu/>) were used as a reference to delineate the remaining orchards. The GIS technique called “heads up digitizing” was used to conduct the pecan delineation.

The orchards were identified as pecans by visual inspection on the true-color DOQQs. The high resolution (1 meter spatial resolution) of the DOQQs allowed for a correct and prompt determination of the crop fields since tree canopies and planting patterns could be observed directly from the aerial photography.

A more effective delineation was achieved by excluding the non-cropped portions of the orchards from the delineations. These non-cropped areas included features such as houses and their surroundings, paved surfaces, barns, machinery, etc.

A total of 1,779 pecan orchards were used in this study to represent individual orchards and to obtain ET estimates from the remote sensing model (Figure 5). Of these orchards, 1,017 were originally from the Doña Ana County database and 762 were manually digitized using the “heads up digitizing” technique.

Average ET values and the number of pixels within each field were obtained for every pecan orchard by superimposing the vector files over the developed ET maps using the region of interest (ROI) tool in ENVI<sup>®</sup> (see Figure 6). The area of each orchard was obtained by multiplying the number of pixels inside the vector by the pixel spatial resolution in each of the maps used (Landsat-7 or ASTER). Additionally, a mosaic of DOQQs with higher resolution (1 meter spatial resolution) covering the entire Valley was used to calculate the area of the orchards and to compare this area to the REEM -ET maps produced with ASTER and Landsat-7 data.

Average ET was calculated for the two datasets (ASTER and Landsat-7) and orchard size groups (*>10 acres* and *<10 acres*) using normal and weighted average methods. The normal average for all vectors (orchards) or normal mean for samples were calculated by summing the pixel average ET values from every vector and dividing it by the total number of vectors. The weighted average was calculated by summing the area of each vector multiplied by the pixel average ET for each vector divided by the summation of the individual areas of the vectors as:

$$\text{Weighted Average ET} = \frac{\sum_{i=1}^n (\text{area of orchard} \times \text{average ET of orchard})}{\sum_{i=1}^n (\text{area of orchard})} \quad (4)$$



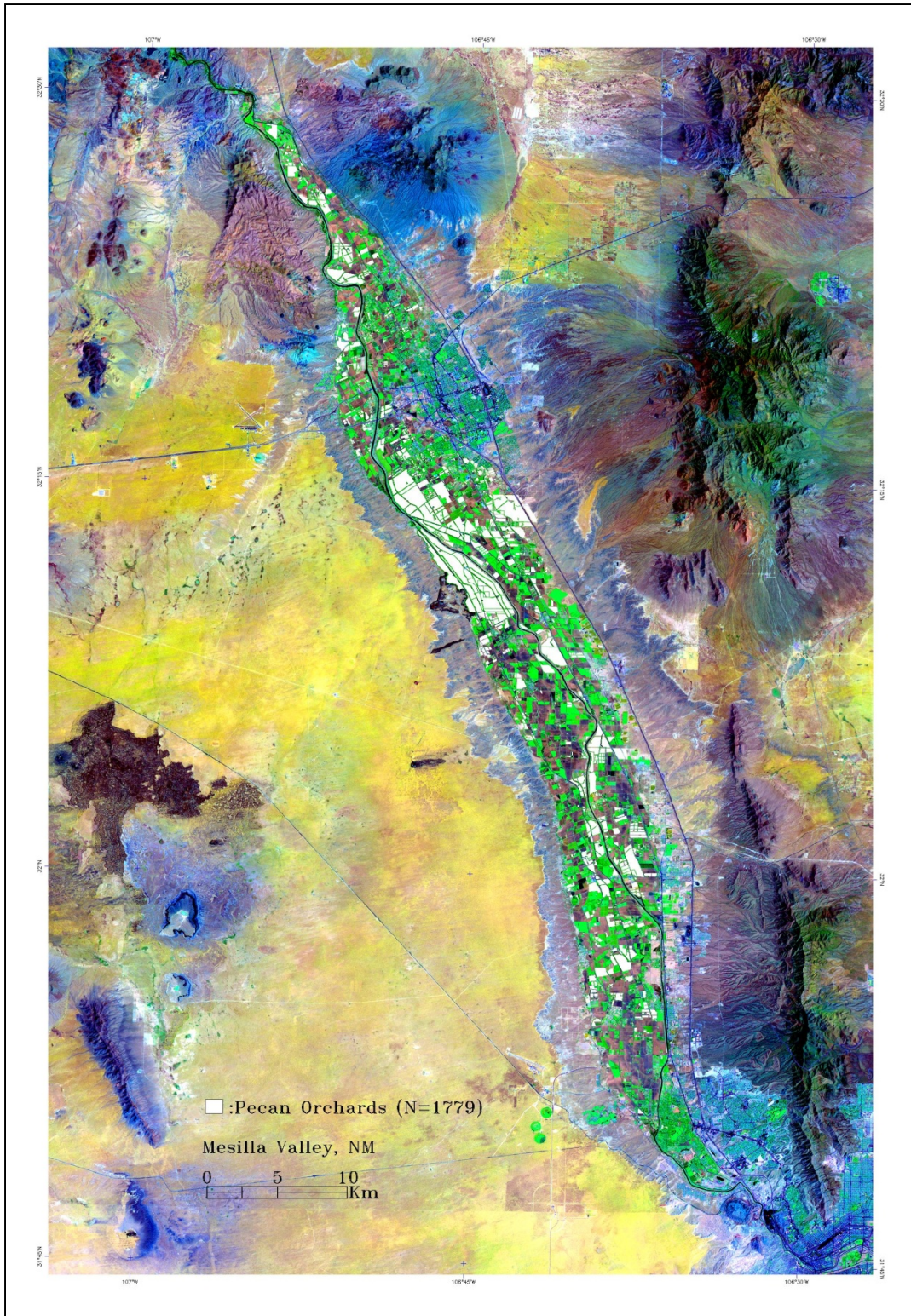


Figure 5. Delineated Pecan Orchards (as White Polygons) in the Mesilla Valley, New Mexico

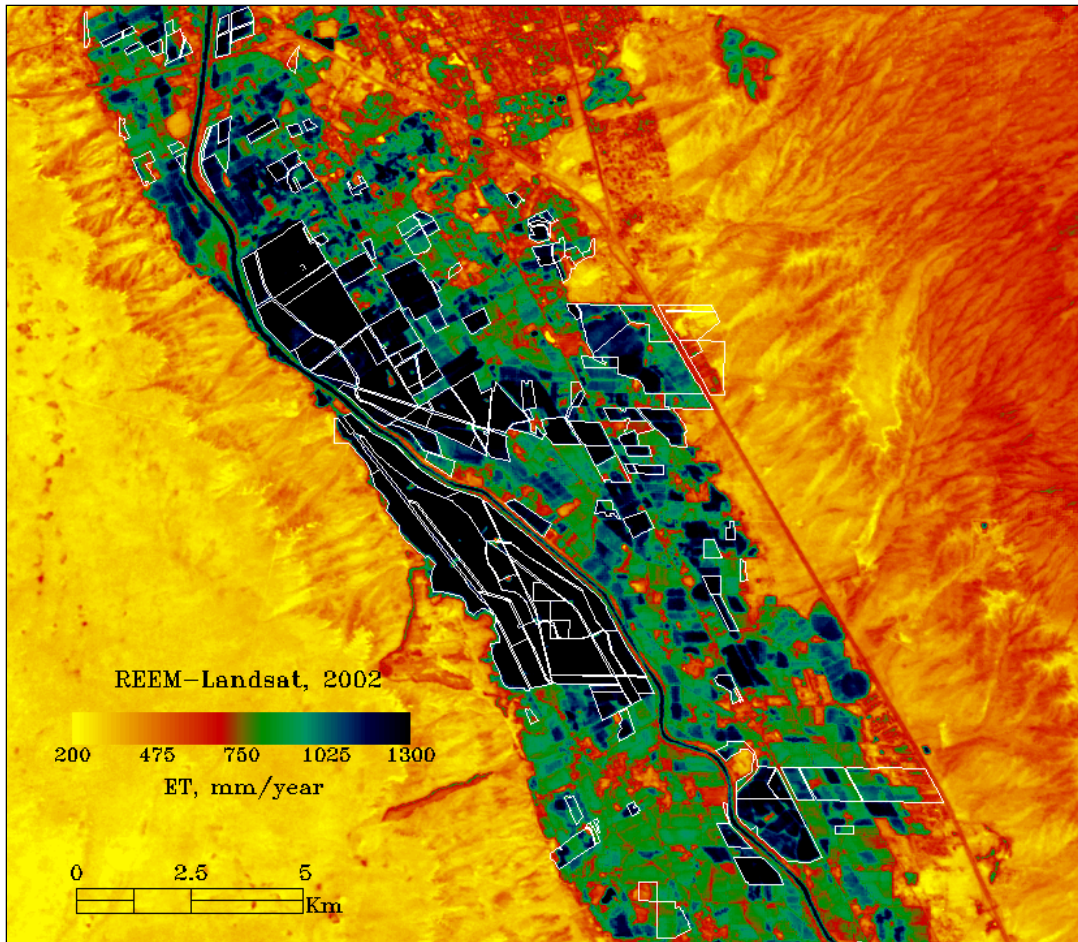


Figure 6. Digitized Vectors of the Pecan Orchards (White Solid Lines) Overlaid in a REEM Annual ET Map by Using the Region of Interest (ROI) Tool in ENVI®

To evaluate spatial and temporal variability of ET, a sample of 280 orchards greater than 4 ha (10 acres) was used to compute annual and monthly ET values. The 280 orchards constituted 66% of the total pecan area within the region of study and were chosen to reduce the impact of the limited spatial resolution of the TIR bands (90 m spatial resolution for ASTER, and 60 m for Landsat-7) in ET estimations. Out of this sample of 280 orchards, plus thirteen small orchards for which fractional cover (fc) measurements were made during the summer of 2007, 170 orchards were used to develop a relationship between fc and vegetation indices (VIs). The number of

orchards used (170 orchards) was limited due to canopy overshadowing effects caused by the position of the sun at the time of acquisition of the aerial photography and in cases where vegetation was growing between the rows of the orchards.

Monthly crop coefficients ( $K_c$ ) were calculated for the orchards as the sum of the daily REEM estimated ET divided by the sum of daily  $ET_{sz}$  for the 30 day period. Sample standard deviation (SD) of orchard ET was calculated as an indication of spatial variability among the orchards.

## 5.2. Estimation of Fractional Cover Using Aerial Photography and Remote Sensing

This section discusses how fractional cover ( $fc$ ) at the orchard level was estimated for 170 pecan orchards using supervised classification of aerial photography. To estimate  $fc$  from remotely sensed data, the values of  $fc$  estimated with supervised classification were related to values of vegetation indices (VIs) calculated from spectral satellite data for 170 pecan orchards. In addition,  $fc$  was measured on thirteen young pecan orchards belonging to a single commercial farm. The field measurements of  $fc$  were then compared to the  $fc$  estimations determined by the supervised classification method.

### 5.2.1. Estimation of fractional cover with supervised classification of CIR-DOQQs

A series of color infrared-DOQQs (CIR-DOQQs) covering the Mesilla Valley area were downloaded from the New Mexico Resource Geographic Information System Program (NM-RGIS) website and used to estimate  $fc$  through digital analysis. Both CIR-DOQQs and DOQQs were acquired from several flights in the Valley

between August 10 and October 1, 2005. The CIR-DOQQs contained three bands from reflectance in the NIR, red and green spectral regions as opposed to the red, green, and blue (RGB) commonly found in true-color digital imagery (Table 3). Reflectance values were in the form of digital numbers (DN).

Before applying the classification technique, the CIR-DOQQs were masked using the vector files and their extent was reduced to cover only the orchard. This procedure helped removing any extraneous radiance data that did not originate in the orchards.

Table 3. Arrangement of Spectral Bands in True-color and Color-infrared DOQQs

Band number	True-color DOQQ		Color-infrared DOQQ	
	Band	Wavelength ( $\mu\text{m}$ )	Band	Wavelength, ( $\mu\text{m}$ )
1	red	0.6-0.7	NIR	0.7-1.1
2	green	0.5-0.6	red	0.6-0.7
3	blue	0.4 -0.5	green	0.5-0.6

Training of the technique consisted of assigning ranges of DN values to defined classes based on knowledge of features in the imagery. The defined classes were “shadows” (approximately from 1 to 60 DN), “tree canopies” (61 to 120 DN) and “bright soil” (120 to 255 DN). Only the red band (band 2 in the CIR-DOQQ arrangement, Table 3) was segmented due to the high light absorption by vegetation, which helped to differentiate between canopies and background. The classification was completed for every masked CIR-DOQQ by adjusting the DN ranges iteratively to ensure that classified images coincided with the original photos. Orchard fc was calculated as the ratio of pixels classified as tree canopies divided by the total number

of pixels in the image. A sample result of a classified CIR-DOQQ is shown in Figure 7.

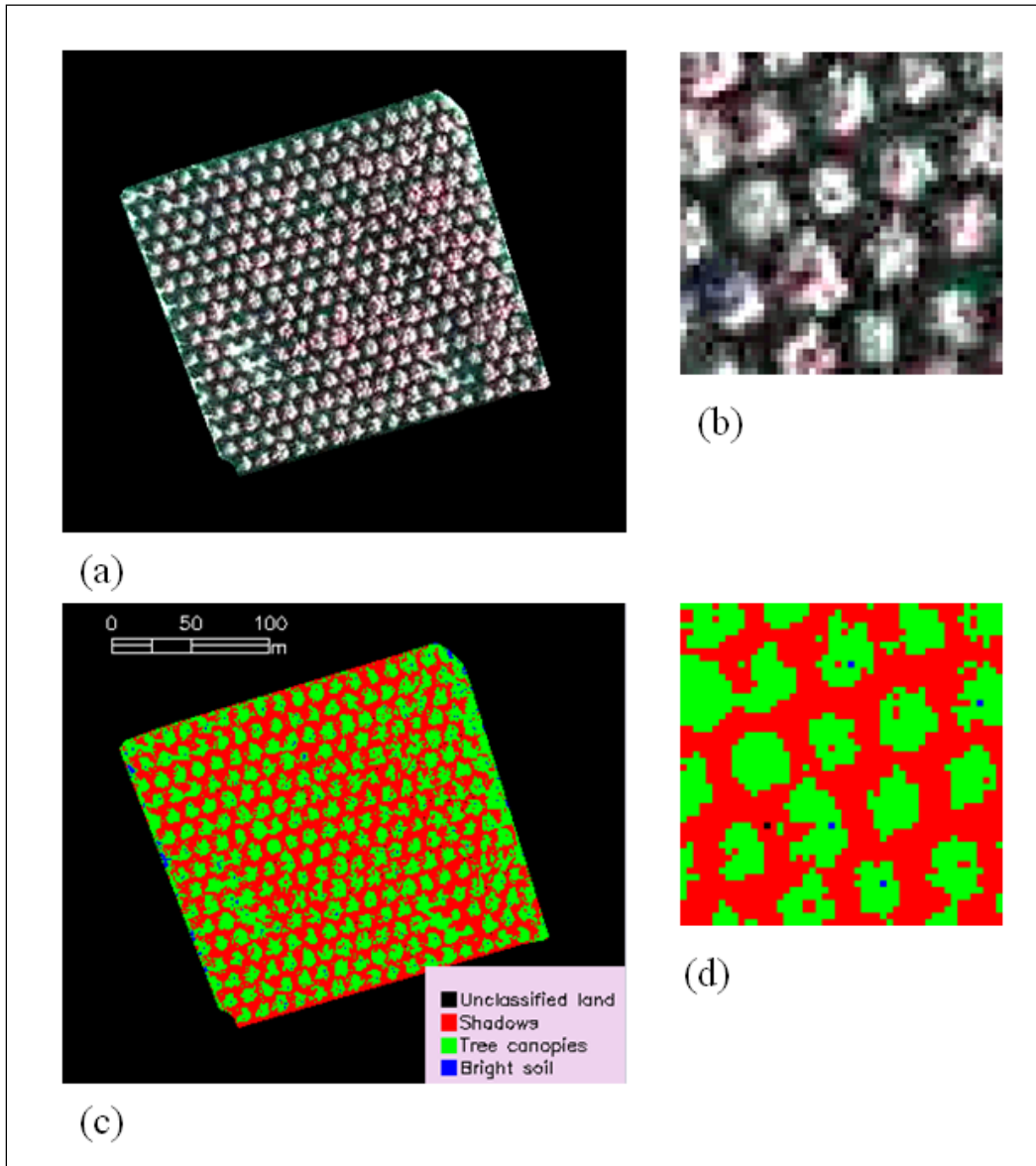


Figure 7. Example of Supervised Classification of a CIR-DOQQ for Estimating Fractional Cover (fc); (a) Masked and subset CIR-DOQQ of a Pecan Orchard, and (b) a Close View of Tree Canopies as Seen from Above; (c) Image After Supervised Classification was Applied and, (d) Close View of the Classified Image to See the Trees in Detail

The masked images for which the “tree canopy” could not be separated from the “shadows” and “bright soil” classes were not considered for determination of  $f_c$  using supervised classification method. In most cases, shadows were caused by the position of the sun at the time of acquisition of the aerial photography since many images were acquired early in the day between 8:00 and 10:00 AM. When the shadows covered a considerable portion of the canopy as seen from above, it resulted in an underestimation of  $f_c$  in the orchard being analyzed. In addition, masked CIR-DOQQs were removed from the analysis when vegetation was growing between the rows of the pecan orchards. This was done since NDVI values for the fields with vegetation were usually higher than for those fields having only pecan trees.

#### 5.2.2. Calculation of vegetation indices

Three different vegetation indices (VIs) were calculated from one ASTER observation in the visible and NIR spectral regions acquired in the late summer of 2005. The three VIs were the normalized vegetation index (NDVI) (Tucker, 1979), the soil adjusted vegetation index (SAVI) (Huete, 1988), and the theta-soil adjusted vegetation index ( $\theta_{SAVI}$ ) (Jiang et al., 2006). The three indices and their respective equations (1-3) were presented in section 2. In the three equations, the NIR reflectance ( $\rho_{NIR}$ ) was the reflectance in band 3 for ASTER and band 4 for Landsat-7, and the red reflectance ( $\rho_R$ ) was the reflectance in band 2 of ASTER and band 3 for Landsat-7. The specific VIs were chosen to avoid saturation problems associated with NDVI (Carlson and Ripley, 1997) as well as the noise created by variations in soil backgrounds and soil type (Huete et al., 1985).

The ASTER observation used for the calculation of VIs was acquired on September 28, 2005 whereas the CIR-DOQQs were taken from aircraft between August 10 and October 1, 2005, a maximum difference of less than two months. Therefore it was assumed that similar conditions in land cover and state of plant growth existed for the orchards when DOQQs and the ASTER observation were acquired.

Landsat-7 spectral data were not available for the time when  $fc$  was estimated from the DOQQs. Therefore, in order to find the relationship between  $fc$  and NDVI computed from Landsat data, a relationship between ASTER and Landsat-7 NDVI for a common date and acquisition time was developed. Two images (ASTER and Landsat-7) acquired on May 15, 2002 at approximately 11:00 AM Mountain Standard Time (MST) were used to calculate the NDVI, and to model the relationship between  $fc$  and Landsat-7 NDVI by calibrating one sensor to the other. Additionally, a matched-pair  $t$  test (Dowdy et al., 2004) was carried out to determine if the values of NDVI calculated with the different sensors (ASTER and Landsat-7) were statistically different.

The 2005 ASTER data also came from the Land Processes Distributed Active Archive Center (LPDAAC). The ASTER data were already corrected for radiometric, geometric and atmospheric conditions (Abrams et al., 2002). Landsat-7 data were corrected for atmospheric conditions present at the time of acquisition. The correction was conducted using the simplified method for the atmospheric correction of satellite measurements in the solar spectrum or SMAC (Rahman and Dedieu, 1994). All satellite imagery were georeferenced individually using a linear polynomial function

with 15 to 20 ground control points (GCPs) extracted from the pecan vector files. Average VI values, number of pixels, and other basic statistics (i.e., maximum, minimum, and standard deviation) in each vector were computed by overlaying the vectors on the transformed VI satellite images by using the Region of Interest (ROI) tool from ENVI<sup>®</sup>.

### 5.2.3. Field measurements of fractional cover

Fractional cover (fc) was measured on thirteen pecan orchards in the summer of 2007. The orchards were part of a 40-hectare commercial farm, located 14 km south of Las Cruces, NM (lat. 32.167° N, long. 106.74° W). The farm was composed of 17 orchards having trees of different ages, row orientation, and tree densities as shown in Figure 8. The trees were 20 or 30 years old with an average height of 9 or 12.5 m, respectively. On May 21 and 22, 2007, when the trees had reached their maximum foliage cover, the fc, trunk diameter, tree density, and tree spacing on the thirteen orchards were measured.



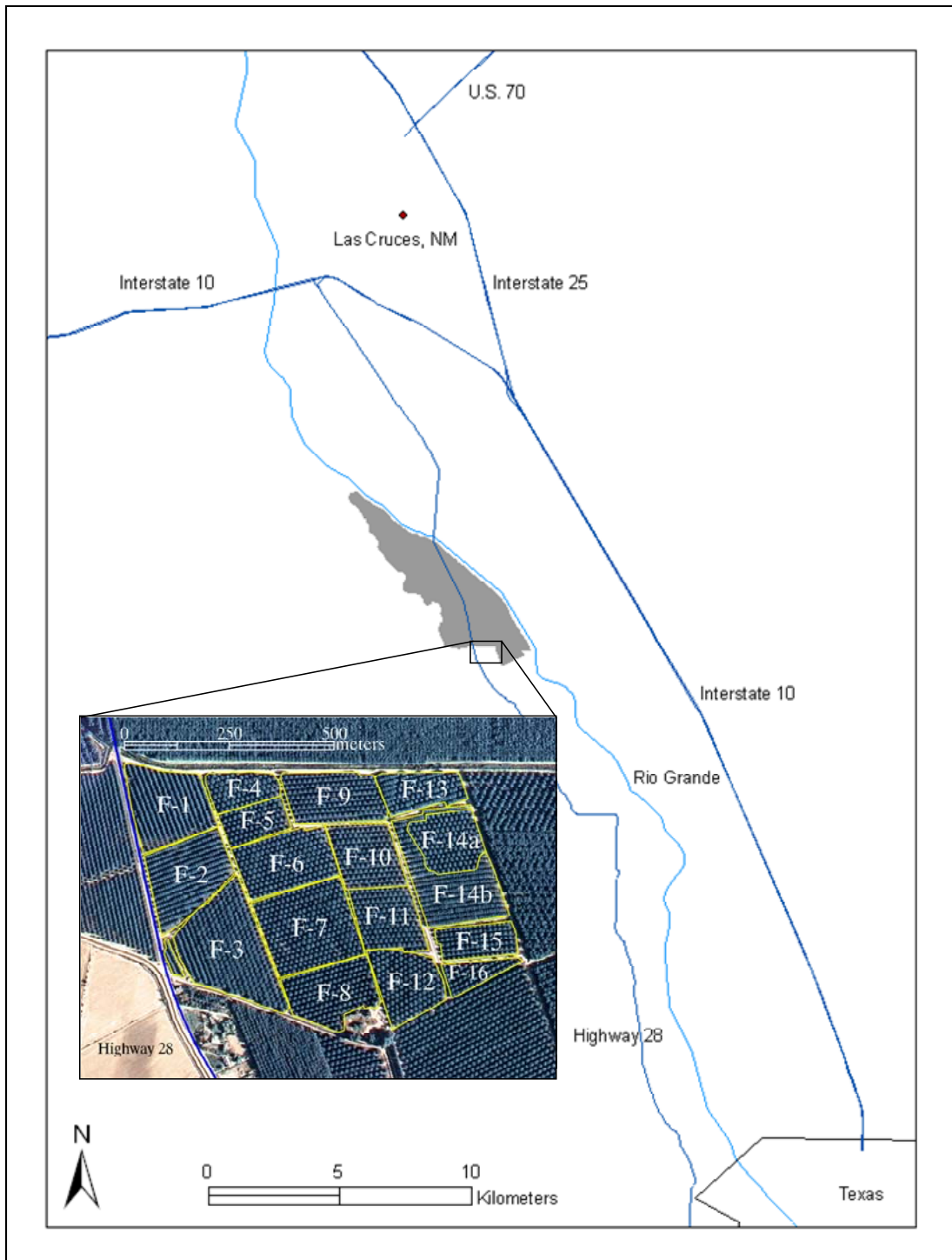


Figure 8. Designation and Spatial Location of the Orchards Measured for  $f_c$  in a Pecan Farm

To determine  $f_c$ , first, all individual trees were identified on aerial maps. In each orchard, a fixed random sample of 25% from the total number of trees was chosen. For each selected tree the distance from the center of the trunk to the end of the canopy (drip line) was measured on the ground. Eight distances or transects were taken every 45° starting from the north direction (0°) below the tree canopy (Figure 9). The canopy areas were found by calculating the area of a circle using the average of the eight transects as a radius. Orchard  $f_c$  was calculated as:

$$f_c = \frac{\text{mean tree canopy area} \times \text{no. trees in orchard}}{\text{area of orchard}} \quad (5)$$

where the mean tree canopy area was equal to the mean tree projected canopy area on the ground for the measured trees in an orchard. Tree spacing was measured on a small number of trees at the site and confirmed later on the geo-referenced DOQQs for all the orchards. Tree density was determined as the number of trees divided by the orchard area.

### 5.3. Development of a Method to Estimate ET from Fractional Cover

One of the main objectives of this study was to develop a methodology to estimate ET from  $f_c$ , a variable that can be easily measured in the field. The first step involved the estimation of  $f_c$  for 170 pecan orchards from the Mesilla Valley using supervised classification of aerial photography (CIR-DOQQs). The results from this method were then compared with field measurements carried out in a commercial farm. The next step was to investigate the relationship between  $f_c$  and some broadly

used VIs (e.g., NDVI) to determine the best-fit equations for estimating  $f_c$  from VIs. Therefore, three VIs were calculated from satellite observations and pecan orchard VI values were related to values of  $f_c$  to develop best-fit equations. With this information, a method to predict ET in pecan orchards was developed by relating annual ET estimated from REEM to pecan  $f_c$  calculated from the NDVI.

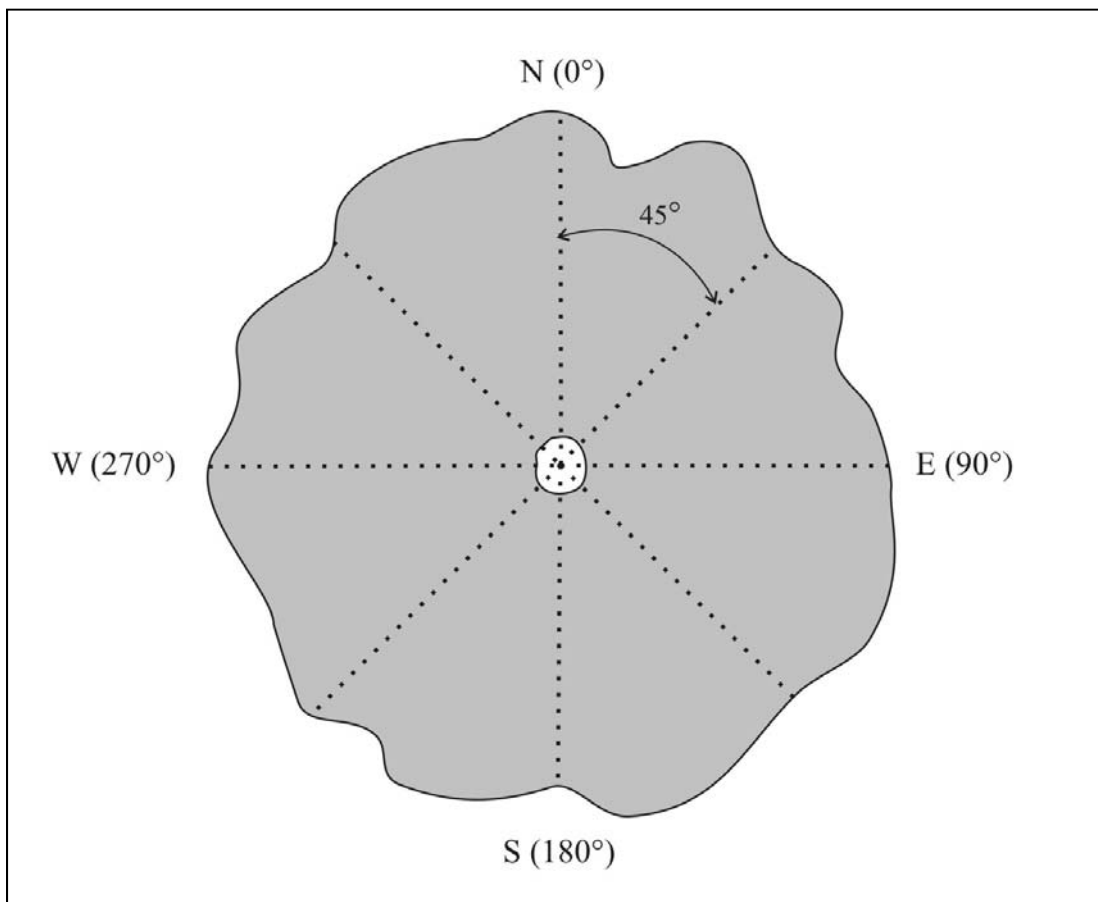


Figure 9. Sketch of the Method Used to Measure the Projected Area of Tree Canopy and  $f_c$ . The dashed lines are the eight transects below the canopy to measure the distance from the center of the trunk to the drip line every 45°.

## 6. RESULTS AND DISCUSSION

### 6.1. Distribution of Acreage among the Pecan Orchards

From the analysis of acreage, using three different base maps (ASTER, Landsat-7, and DOQQ mosaic), it was found that the majority of the pecan orchards in the Mesilla Valley were small fields of less than 4 ha (10 acres) in size. The orchards smaller than 10 acres constituted 76% of all the pecan orchards in the Valley but only accounted for only 19% of the total land planted with pecans. Conversely the orchards greater than 10 acres constituted only 24% of all orchards but accounted for 81% of the total pecan area (Table 4). The total area planted with pecans in Mesilla Valley as projected in the DOQQ mosaic was 9,753 ha (24,101 acres).

The projected area and number of orchards included in each classified group (*>10 acres* and *< 10 acres*) were probably affected by both the ground resolution of the map and the sensor resolution. The area of the orchards obtained with the DOQQ mosaic was used to validate areas obtained with the ET maps from ASTER and Landsat-7 satellite data. The DOQQs were considered more accurate due to the higher spatial resolution of one meter. The ASTER and Landsat-7 map coarser resolutions of 15 m and 30 m tended to overestimate the area as compared to the DOQQ mosaic. As a result of lower (coarser) resolution, overlaying the vectors on the Landsat-7 ET map yielded more orchards in the *>10 acres* category (433) as compared to the DOQQ mosaic (420). See Table 4.

Table 4. Differences in Acreage and Number of Pecan Orchards Using Three Different Maps

Map	Orchards > 10		Orchards < 10		Total no. orchards	Total acreage	Diff. from DOQQ
	No.	Acreage	No.	acreage			
Landsat <sup>a</sup>	433	19,929 (8,068 ha)	1,346	4,626 (1,873 ha)	1779	24,555 (9,941ha)	1.9%
ASTER <sup>b</sup>	424	19,562 (7,920 ha)	1,354	4,574 (1,852 ha)	1778 <sup>c</sup>	24,277 <sup>d</sup> (9,829ha)	0.7 <sup>d</sup> %
DOQQ <sup>e</sup>	420	19,582 (7,928 ha)	1,359	4,519 (1,830 ha)	1779	24,101 (9,758ha)	0.0%

<sup>a</sup>Spatial resolution is 30 meters; <sup>b</sup>Spatial resolution is 15 meters; <sup>c</sup>One vector was excluded from the REEM-ASTER annual ET map due to differences in the extent of the map compared to Landsat-7; <sup>d</sup>Area after adding the acreage of the missing vector; <sup>e</sup>Spatial resolution is 1 meter

The 2007 Census of Agriculture reported a total area for pecans in Doña Ana County of 11,047 ha (27,298 acres) by the end of 2006 (NASS, 2010). This represents 11.2% more acreage than that determined with the DOQQs (9,758 ha or 24,101 acres). The difference between the two estimates could have been due to the differences in the delineation of the region analyzed in this study and/or due to methodology of survey conducted by the 2002 Census of Agriculture. The delineated area for this study was smaller than the County area.

Figure 10 shows the distribution of sizes for all the pecan orchards in the Valley as projected in the DOQQ mosaic. The minimum area found for an orchard was 0.12 ha (0.3 acres), the maximum was 208 ha (513 acres) and the average for all the orchards was 5.5 ha (13.5 acres).

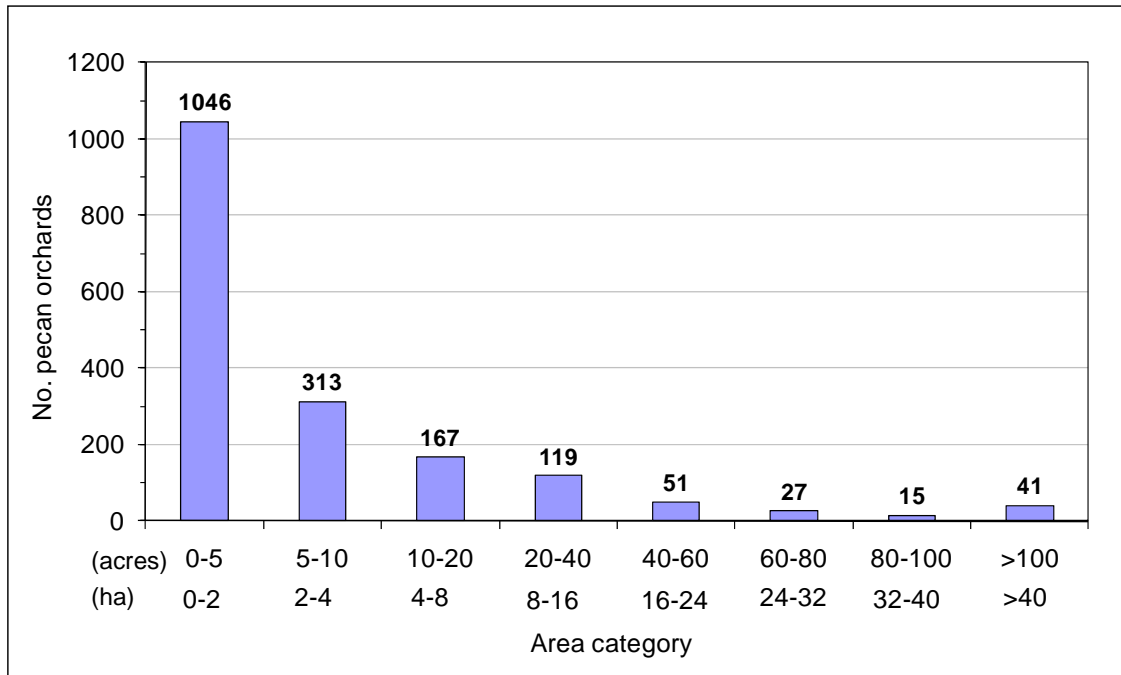


Figure 10. Distribution of Area for 1,779 Pecan Orchards in the Mesilla Valley as Projected in the DOQQ Mosaic

## 6.2. REEM Estimated Pecan ET

The ET maps created with two different satellite data (ASTER and Landsat-7) depicted a high spatial and temporal variation of ET in the Valley as shown in Figure 6. By overlaying the vectors (orchards) over the annual ET maps, the results showed that pecan ET estimated using Landsat-7 data in the REEM was higher than using ASTER data. The Landsat-based annual ET map resulted in a weighted mean annual ET of 1,018 mm and 852 mm for the orchards greater than 10 acres and less than 10 acres, respectively. For the ASTER-based annual ET map, the weighted mean annual ET was 991 mm for the orchards greater than 10 acres and 800 mm for those less than 10 acres. When computed for all the orchards together (n = 1,779), the weighted average annual ET was 955 mm using ASTER data and 987 mm using

Landsat-7 data (Table 5). The maximum annual ET estimated for an individual orchard with the ASTER ET map was 1,307 mm, while for Landsat-7 the maximum was 1,260 mm. The lowest annual ET value found for an orchard using ASTER data was 296 mm, and 368 mm using Landsat-7 data. A histogram of annual ET for all the pecan orchards from the Valley is shown in Figure 11.

Table 5. Weighted Annual Average or Mean ET for the Pecan Orchard Categories Using the ASTER and Landsat-7 Data Sets

Satellite Data	All orchards	> 10 acres	< 10 acres
	weighted average or mean ET, mm/yr		
ASTER	955	991	800
Landsat-7	987	1,018	852

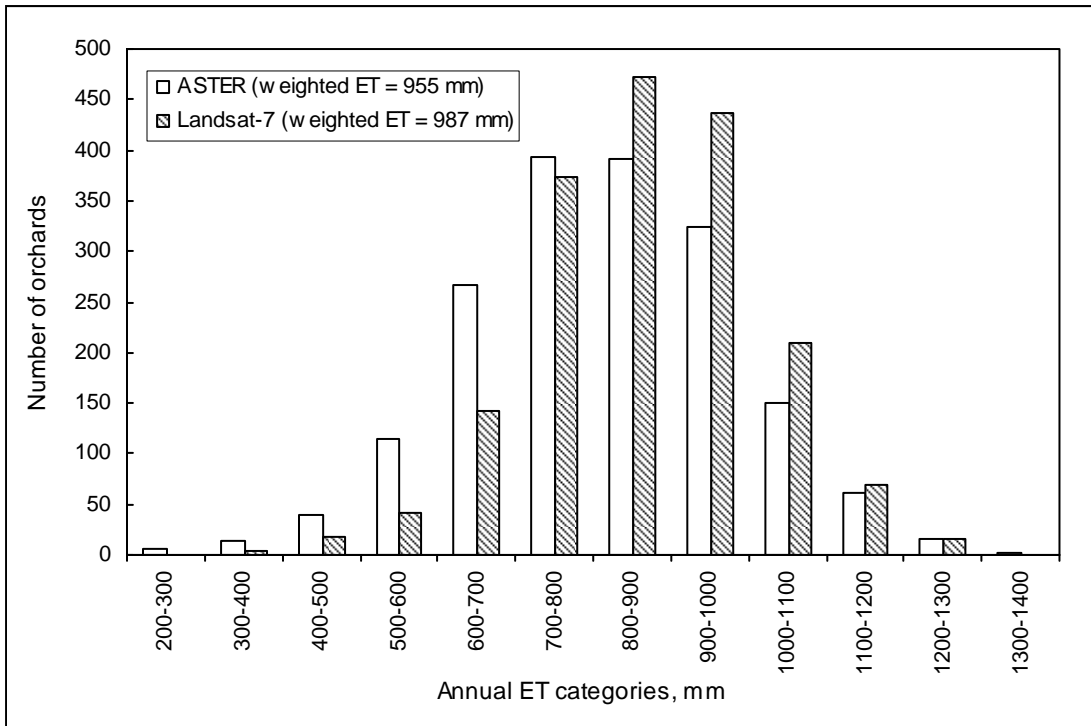


Figure 11. Histogram of Annual ET for All the Pecan Orchards (n = 1,779 and 1,778) Using ASTER and Landsat-7 Data During 2002

Differences in ET results using the ASTER and Landsat-7 data were probably due to the availability of more clear-sky satellite scenes during the year for Landsat-7 than for ASTER (Table 2). This could have affected the daily Kc estimation due to interpolation between the less frequent ASTER scenes. The Landsat-7 data set had more clear sky spectral observations and therefore ET values obtained from the REEM-Landsat were considered to be more reliable than those obtained with the limited (sparse) ASTER data.

Differences in the REEM modeled ET values compared to measured values and between the two satellites data were also due to the impact of coarser resolution of the thermal infrared (TIR) bands. The TIR pixel size for ASTER is 90 m while for Landsat-7 is 60 m. The ET values in pixels near the boundaries of a field are affected by other conditions such as oasis effect outside the pecan fields. This caused the estimated parameters in pixels near the boundaries to be lower than expected. The effect was more pronounced in smaller fields that were less than 10 acres or 4 ha. The impact of the boundary effect was higher in the ASTER produced ET maps than in the Landsat-7 produced ET maps.

Table 6 shows statistics for monthly ET from the sample of 280 pecan orchards. The standard deviation (SD) of vector ET was calculated in order to determine the variability in ET among the orchards during the year. The variability in ET estimates was consistently higher when using ASTER data when compared to Landsat-7 data. This was possibly due to the lack of continuous cloud-free satellite images from ASTER. In both ASTER and Landsat-7 monthly ET generated maps, the highest ET variation occurred in May (ASTER, SD = 28.4 mm/month and Landsat-7,



SD = 27.13 mm/month). The highest SD for the month of May could be attributed to early spring leaf development. In general, the variability of ET among orchards was higher from April to September as shown in Table 6. This corresponds to the growing season.

Table 6. Statistics for Mean Monthly ET for 280 Pecan Orchards Using ASTER and Landsat-7 Data During 2002

Month	Minimum	Maximum	Mean	Weighted mean	SD
REEM-ASTER					
January	0.01	26.96	13.52	15.44	5.82
February	0.11	34.45	17.88	20.30	7.22
March	2.87	80.41	48.72	54.06	14.76
April	19.16	129.59	85.48	93.60	21.13
May	43.64	187.74	128.39	139.72	28.40
June	52.72	203.28	144.96	157.63	27.75
July	85.19	188.77	147.31	157.01	20.17
August	72.60	184.18	146.76	156.29	19.53
September	52.61	130.54	102.76	110.03	15.00
October	23.98	89.71	68.85	74.17	11.06
November	4.55	53.15	36.40	39.54	7.87
December	0.21	17.28	9.37	10.58	3.45
REEM-Landsat-7					
January	7.45	26.07	17.53	18.75	2.88
February	11.15	31.82	23.42	24.79	3.53
March	26.90	88.84	53.07	55.61	9.91
April	26.13	116.43	77.65	84.18	17.47
May	39.42	173.95	120.45	132.40	27.13
June	87.34	210.53	167.77	179.75	24.87
July	72.65	180.90	146.19	155.12	19.75
August	81.57	186.26	149.54	158.11	18.78
September	70.55	155.25	125.93	132.39	14.72
October	31.62	82.32	66.10	69.42	8.34
November	16.07	39.58	30.82	32.56	3.99
December	4.62	15.56	10.61	11.34	1.70

Figure 12 shows annual ET using Landsat-7 data as function of field size for 1,779 orchards during 2002. As shown in Figure 12, smaller orchards had a greater variation in annual ET as compared to larger orchards. This could be due to boundary processes such as oasis effects or impact of coarser resolution of the thermal infrared pixels (edge effect), which are more pronounced in orchards smaller than 10 acres.

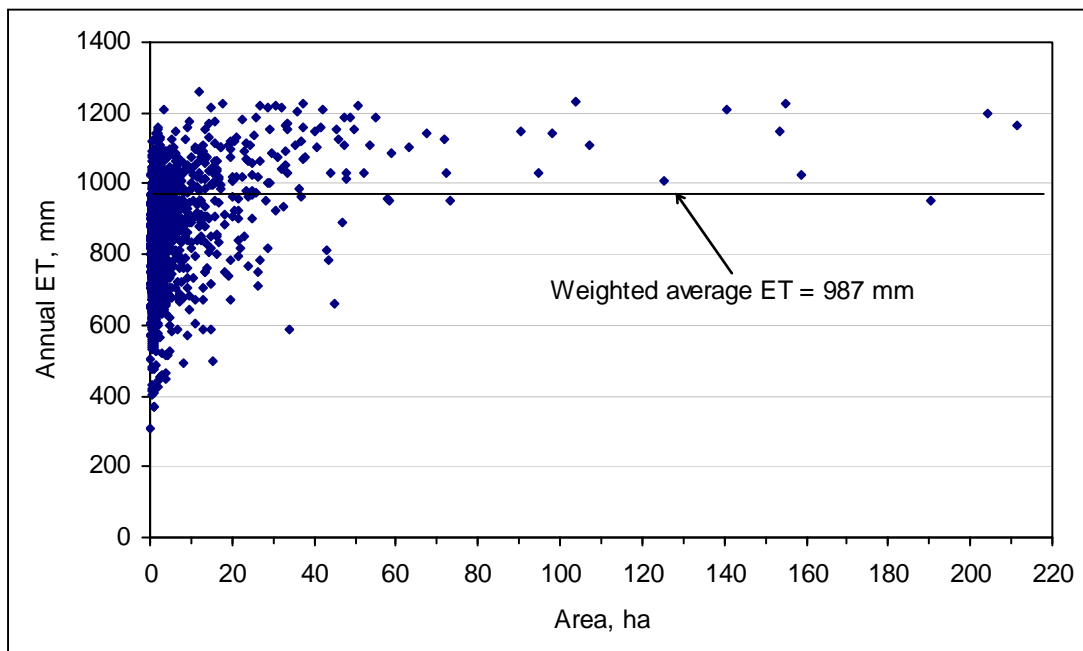


Figure 12. Relationship between Orchard Size and Annual ET for 1,779 Pecan Orchards in the Mesilla Valley Using 2002 Landsat-7 Data

### 6.3. Comparison of Estimated Pecan ET and ET Published in Literature

Table 7 shows a comparison between seasonal ET estimated with Landsat-7 and ASTER-based ET maps and published values for pecans. The ET values using ASTER and Landsat-7 ET maps were computed for two circular vectors having different number of pixels superimposed in the vicinity of the ET flux tower installed

in a mature pecan orchard. The instrumentation of the ET flux tower and study site were described in detail by Samani and others (2009). The estimates using ASTER and Landsat-7 compared well with measurements reported by other researchers, except for July and August when the values were slightly lower than those from the literature. The seasonal (April-November) ET obtained with REEM using ASTER data was 1,186 mm and using Landsat-7 was 1,217 mm. Seasonal values reported by other authors ranged from 1,173 to 1,307 mm (Table 7). The ET values for pecans obtained in the proximity of the flux tower were within the range of the values published in literature.

Table 7. Comparison of Seasonal ET Estimated with Landsat-7 and ASTER Data Compared with Those Published in Literature

Month	2002 <sup>a</sup>	2002 <sup>b</sup>	2001 <sup>c</sup>	2002 <sup>c</sup>	2004 <sup>d</sup>	Long-term <sup>e</sup>
ET, mm						
April	130	118	88	136	106	70
May	187	192	177	176	184	119
June	203	217	202	218	225	225
July	187	181	221	199	227	278
August	186	190	210	198	207	290
September	147	159	185	170	154	239
October	92	93	136	73	106	86
November	54	66	40	3	46	----
Total	1,186	1,217	1,259	1,173	1,255	1,307

<sup>a</sup> ASTER-REEM ET estimated at the flux tower site, n = 1,898 pixels, area = 0.43 km<sup>2</sup>

<sup>b</sup> Landsat-REEM ET estimated at the flux tower site, n = 289 pixels, area = 0.26 km<sup>2</sup>

<sup>c</sup> Sammis and others (2004) measured from April 1-November 20 in 2001 and April 1-November 6 in 2002

<sup>d</sup> Reveles (2005)

<sup>e</sup> Miyamoto (1983) estimated from April 1 to October 15 for a long-term period at El Paso, TX

#### 6.4. Estimation of Fractional Cover in the Pecan Orchards

In order to evaluate the performance of the supervised classification of color infrared-Digital Ortho-photo Quarter-Quadrangles (CIR-DOQQs) to estimate

fractional cover (fc), the results obtained with this method were compared to the field measurements carried out in the thirteen young orchards. Only thirteen orchards in the Valley were used to test this methodology due to limited resources at the time of the study. However, a larger sample of field measurements of orchards randomly selected within the Valley is recommended. A total of 170 orchards, which included thirteen young pecan orchards that were measured for fc in the summer of 2007, were analyzed to develop a relationship between fractional cover (fc) and vegetation indices (VIs).

Fractional cover values obtained with the supervised classification method in the 170 masked CIR-DOQQs ranged from 13% to 74% with a mean of 54% as shown in Figure 13. The fc values measured in the thirteen young pecan orchards ranged from 34% to 76% with a mean of 53%. Table 8 shows the values of fc and the field variables measured for the thirteen orchards. Table 9 compares the estimated (supervised classification of CIR-DOQQs) and measured fc values in 2005 and 2007 respectively. The average absolute difference between the two methods of supervised classification and field measurements was 7% (fc is expressed as percentage) and the average percentage error between the two methods was calculated as 14%. The estimated 2005 fc values were consistently smaller than the values measured in 2007. Differences can be explained by the growth of the trees over the two year period, management practices such as pruning of trees, and some error in the estimation of fc with the supervised classification method. Nevertheless, in order to validate the supervised classification method, a larger number of field measurements of fc needs to be undertaken at a time closer to the satellite overpass. Furthermore, the field

measurements need to be carried out in orchards displaying differences in tree age and size, densities (spacing), fc, and under different management practices.

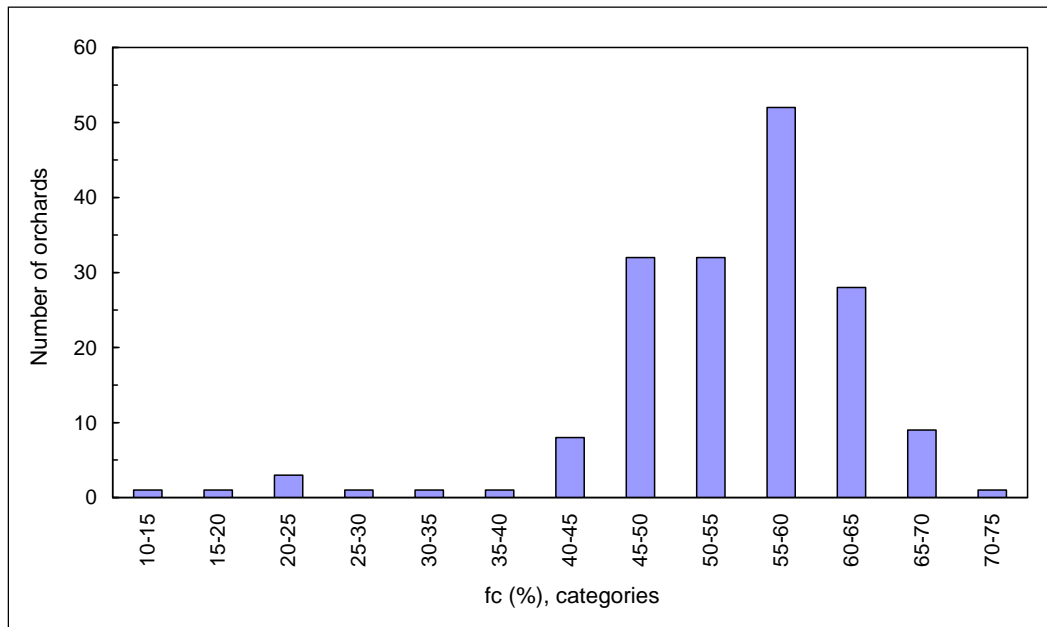


Figure 13. Histogram of fc Values Estimated with the Supervised Classification Method for 170 Pecan Orchards During 2005

Table 8. Measured Field Parameters of Thirteen Pecan Orchards

Field	No. trees	Field area (ha) <sup>a</sup>	fc (%)	Spacing (m) <sup>a</sup>	Avg. trunk diameter (cm)	Tree density (tree/ha)
F-1 <sup>b</sup>	418	3.08	65.07	6.1 x 12.2	20.8	136
F-2 <sup>b</sup>	413	3.13	71.51	6.1 x 12.2	19.0	132
F-4	85	1.30	47.68	11.6 x 13.7	32.8	66
F-5	86	1.30	44.31	11.6 x 13.1	25.9	68
F-6	198	2.95	49.41	11.9 x 13.7	30.7	67
F-7	280	4.26	35.74	12.8 x 13.7	35.8	66
F-8	173	2.67	62.34	12.3 x 13.7	31.1	65
F-10	155	2.30	33.85	13.1 x 13.4	28.6	68
F-11	151	2.23	53.05	12.2 x 13.7	28.8	66
F-12	154	2.35	49.66	12.2 x 13.7	34.4	65
F-14a	128	1.96	54.41	12.2 x 13.7	25.3	65
F-15	109	1.47	43.55	11.9 x 11.6	33.0	76
F-16	61	0.88	75.63	12.2 x 13.1	41.2	68

<sup>a</sup> Determined from high resolution DOQQ

<sup>b</sup> Fields with younger trees of 20 years old and rectangular arrays; the remaining fields had an average age of 30 years and staggered or offsetting arrays

Table 9. Measured Versus Estimated fc in Thirteen Pecan Orchards

Field	Measured fc, % (May 2007)	Estimated fc, % (Aug-Oct 2005)	Absolute difference, %	Percent error
F-1	65.07	57.86	7.21	11.08
F-2	71.51	62.83	8.68	12.13
F-4	47.68	53.84	6.15	12.91
F-5	44.31	44.37	0.06	2.14
F-6	49.41	49.02	0.40	0.81
F-7	35.74	44.83	9.08	25.41
F-8	62.34	48.29	14.05	22.54
F-10	33.85	49.07	15.22	46.27
F-11	53.05	49.68	3.37	6.35
F-12	49.66	45.35	4.30	8.66
F-14a	54.41	49.20	5.21	9.57
F-15	43.55	48.97	5.42	12.45
F-16	75.63	64.95	10.69	14.13
Average	52.79	51.40	6.91	13.93

#### 6.5. Relationship between Fractional Cover and Vegetation Indices

In order to find the relationship between fc and VIs, simple linear regression analyses were undertaken between estimated fc and VIs from the ASTER observation acquired on September 28, 2005. The NDVI had the highest correlation with fc ( $R^2 = 0.709$ ) followed by  $\theta_{SAVI}$  ( $R^2 = 0.689$ ) and SAVI ( $R^2 = 0.685$ ). The use of the indices SAVI and  $\theta_{SAVI}$  did not improve the relationship of NDVI with fc as suggested by the literature. The three relationships were statistically significant ( $p < .001$ ) after an analysis of variance (ANOVA) for linear regression was performed to test the significance of the relationships. Table 10 presents linear regression statistics for the relationships between fc and the mentioned VIs. The statistics presented in Table 10 are the slope, a, and intercept, b, of the linear equations, coefficient of determination ( $R^2$ ) and adjusted coefficient of determination ( $R^2$  adjusted), the standard error of estimate (SEE) and the  $F$  value calculated for the

ANOVA. The calculated  $F$  values were sufficiently high to reject the null hypothesis that slope of the linear equation is zero.

Table 10. Linear Regression Statistics for Estimating  $fc$  from NDVI, SAVI and  $\theta_{SAVI}$

Independent variable	Slope a	Intercept b	$R^2$	$R^2$ adjusted	SEE	$F$
NDVI	1.202	-0.061	0.709	0.707	0.0499	408.98
SAVI	0.780	-0.043	0.685	0.684	0.0519	366.12
$\theta_{SAVI}$	0.710	-0.111	0.689	0.687	0.0516	372.16

NOTE. All three relationships were statistically significant under the ANOVA ( $p < .001$ )

The relationship between  $fc$  and NDVI is shown in Figure 14. In this figure, the function of the linear regression to determine  $fc$  from ASTER-NDVI ( $NDVI_{ASTER}$ ) is presented in equation 6:

$$fc = 1.202 \times NDVI_{ASTER} - 0.061 \quad (6)$$

The large scatter shown in Figure 14 was probably caused by partial mixing of segmented classes in some masked CIR-DOQQs, biases introduced by the observer separating the classes, and possibly edge effect caused by the ground resolution of the NDVI image (15 m spatial resolution). Edge effect may have caused lower NDVI values in or near the boundaries of orchards increasing the variability in the developed  $fc$  vs. NDVI relationship. This phenomenon was also discussed by several researchers (Clark et al., 2007; Tasumi et al., 2005; Markham, 1985) and is starting to gain attention, particularly in agricultural studies that deal with parameters retrieved from satellite observations.

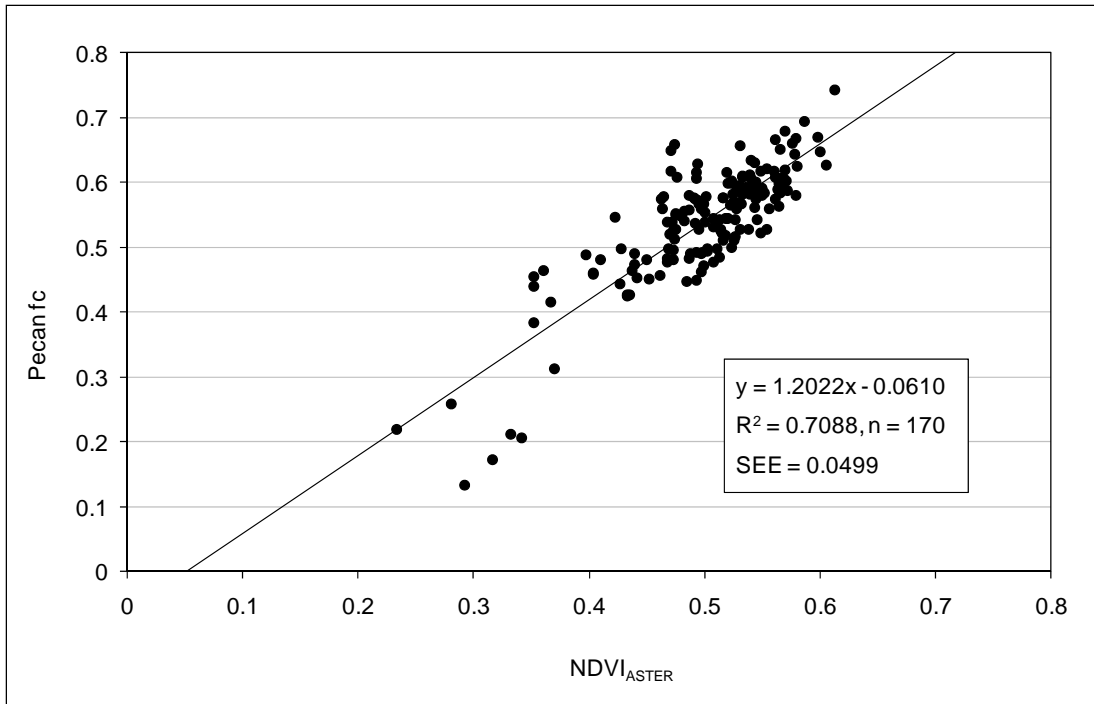


Figure 14. Linear Relationship between fc and NDVI for 170 Pecan Orchards in the Mesilla Valley from an ASTER Image Acquired on September 28, 2005

In regard to the comparison between NDVI computed from ASTER and Landsat-7 data, the matched-pair  $t$  test concluded that both NDVI values were significantly different ( $t = 40.5, n = 280$  pecan orchards,  $p < 0.005$ ) since Landsat-7 NDVI ( $NDVI_{Landsat}$ ) values were on the average 25% higher than ASTER NDVI ( $NDVI_{ASTER}$ ). Figure 15 presents the linear relationship between NDVI from ASTER and Landsat-7 data acquired on the same day at a close time for a sample of 280 pecan orchards. As shown in Figure 15, a linear relationship between  $NDVI_{Landsat}$  values and  $NDVI_{ASTER}$  was developed:

$$NDVI_{Landsat} = 1.253 \times NDVI_{ASTER} + 0.0018 \quad (7)$$



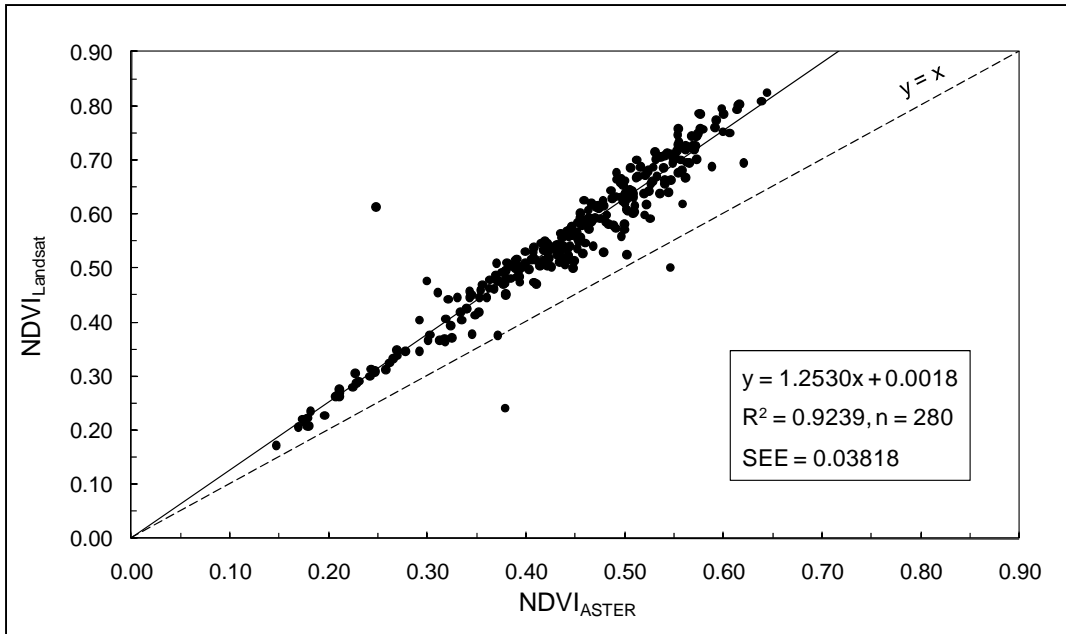


Figure 15. Linear Relation between  $NDVI_{Landsat}$  and  $NDVI_{ASTER}$  Values Obtained for 280 Pecan Orchards in the Mesilla Valley from an Observation Made on May 15, 2002

The relationship between  $fc$  and  $NDVI$  using Landsat-7 data was found after transforming the  $NDVI_{ASTER}$  values into  $NDVI_{Landsat}$  using equation 7 and plotting these transformed  $NDVI$  values with values of  $fc$ . Figure 16 shows the relationship between  $fc$  and  $NDVI_{Landsat}$ . From Figure 16, the linear regression equation to calculate  $fc$  from  $NDVI_{Landsat}$  is:

$$fc = 0.960 \times NDVI_{Landsat} - 0.063 \quad (8)$$

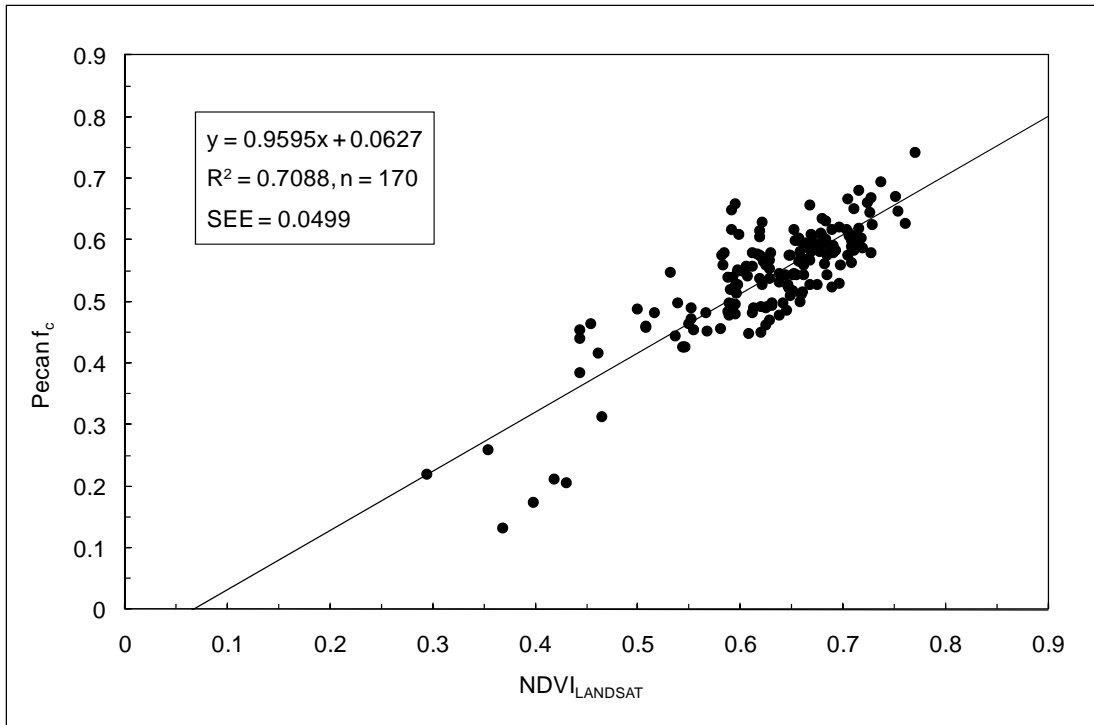


Figure 16. Relationship Between  $f_c$  and ASTER NDVI Converted to Landsat-7 NDVI Using Equation 7 for 170 Pecan Orchards in the Mesilla Valley on September 28, 2005

#### 6.6. Predicting ET as a Function of Midseason NDVI and Fractional Cover

Linear regression was used to analyze the relationship between  $K_c$  and NDVI for the sample of 280 pecan orchards using  $K_c$  and NDVI values during 2002 when satellite data were available (data not shown). It was noticed that the relationship between  $K_c$  and NDVI differed throughout the year from having no correlation during the non-growing season to a strong linear relationship during the individual months of growing season. Therefore no unique relationship between  $K_c$  and NDVI was found that could be used as a predictive model in pecans for the entire growing season. For that reason an alternate procedure that relates a single NDVI calculated

during the middle of the season to the annual ET of pecans was developed to create a methodology for estimating ET from fc via NDVI.

Prediction of ET from midseason NDVI was based on research initially established by Groeneveld and others (2007). They stated that in arid and semi-arid climates the largest consumptive use occurs in the middle of the growing season. This also coincides with the time of maximum leaf area development for most plants in these environments (Or and Groeneveld, 1994). Since the NDVI can be related to photosynthetic activity (Tucker, 1979) and leaf conductance in plants, the NDVI can be used as an indication of the amount of water use or ET (Groeneveld et al., 2007).

Groeneveld and others (2007) used the NDVI\*, an adjusted NDVI for maximum (canopy saturation) and minimum NDVI (bare soil condition) values found in a satellite image, as the predictor for the ET of vegetation on an annual basis. Groeneveld and others (2007) paired the NDVI\* from single Landsat observations acquired in the midseason with total annual ET measurements made with micrometeorological methods (i.e., eddy covariance and Bowen ratio) in different locations. According to Groeneveld and others (2007), the NDVI\* was found to be an effective predictor for annual ET in different plant ecosystems, climates and patterns of growing seasons.

Following Groeneveld and others (2007), midseason NDVI calculated from a single Landsat-7 image on June 16, 2002 was used as indicator of the annual ET for the pecan orchards in the Mesilla Valley. However the standard NDVI was used instead of the NDVI\* suggested by Groeneveld and others (2007). The midseason NDVI was plotted against the annual ET for 280 orchards using the Landsat-based

REEM-ET maps. Annual ET was strongly correlated to midseason NDVI ( $R^2 = 0.73$ ) as shown in Figure 17. This approach however was not used in the ASTER-based REEM-ET maps due to lack of satellite imagery during the months of June and July and presence of clouds in the image of August 19, 2002. Equation (7) was used to convert Landsat-7 NDVI values to  $f_c$ , a measurable variable on the field scale. Figure 18 shows the linear relation between pecan annual ET and  $f_c$  computed from NDVI for the midseason ( $R^2 = 0.73$ ).

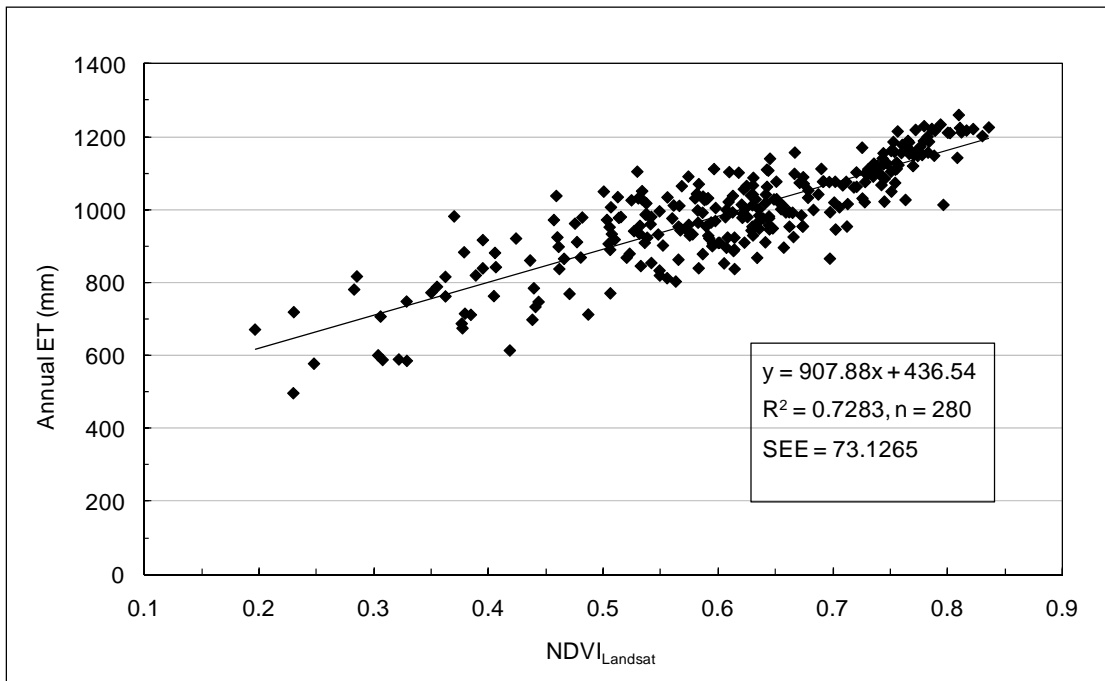


Figure 17. Linear Relation between Midseason NDVI from a Landsat-7 Scene from June 16, 2002 and REEM Annual ET for 280 Pecan Orchards in the Mesilla Valley

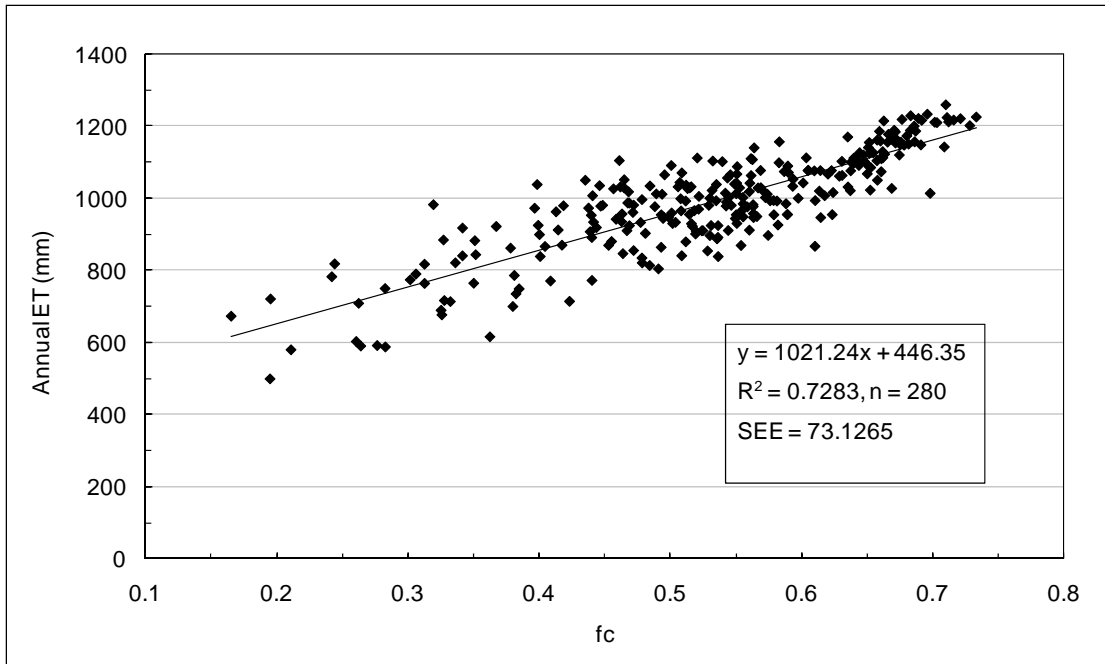


Figure 18. Linear Relation between Midseason  $fc$  Calculated from an NDVI Image for June 16, 2002 and REEM Annual ET for 280 Pecan Orchards in the Mesilla Valley

The developed relationships shown in Figures 17 and 18 allow the estimation of annual ET values for pecan orchards in the Mesilla Valley as a function of midseason NDVI or  $fc$ . However, it should be noted that the linear equations developed from these relationships represent the conditions of a large number of orchards from the area of study and includes stressed and non-stressed orchard ET values. These relationships (NDVI and  $fc$  vs. ET) need to be compared with field measurements of ET and  $fc$  of several pecan orchards of different ages, canopy densities, and management practices to determine their validity.

The importance of the developed relationship based on midseason NDVI or  $fc$  is that it allows estimation of annual pecan ET on a field basis for an entire region by using a single satellite image (NDVI) during the middle of the season. The spectral

observation from the visible and NIR spectral regions to calculate NDVI can be acquired from any operational satellite (i.e., ASTER, Landsat, etc.) or from an aerial multispectral camera. Spectral observations from the Valley can be taken with a multispectral camera from various flights scheduled every summer (around June 15) to predict annual pecan ET for the next season with the method established here. Using this methodology, state and county agencies can predict seasonal ET before the next irrigation season starts in order to make decisions on water budgets and allocation plans to distribute water more efficiently within the Mesilla Valley. A required assumption in the procedure is that there are no significant differences in  $f_c$  from one season to another, which may not be true in young and rapidly growing orchards.

## 7. SUMMARY AND CONCLUSIONS

### 7.1. Summary

An analysis that involved the use of GIS vector files, ET maps created with a remote sensing model (REEM) that used satellite data from two different sensors (ASTER and Landsat-7), weather data, and measured ET during 2002 was undertaken to study the spatial variation of ET among pecan orchards in the Mesilla Valley, New Mexico. The main objective of this study was to evaluate water use (ET) of the pecan orchards in the Mesilla Valley and to relate pecan ET to the vegetation fractional cover (fc) in order to develop a methodology to predict ET from fc which can be measured in the field. The results from this study indicated that the ET in pecans exhibited a high spatial and temporal variation among the orchards of the region. In addition, a linear relationship was developed between pecan fc and the normalized vegetation index (NDVI) calculated from ASTER and Landsat-7 data. From these relationships another linear relationship was developed that could estimate pecan orchard ET based on mid-season fc.

### 7.2. Conclusions

Regional pecan ET in the Mesilla Valley, New Mexico was evaluated using satellite remote sensing, and a relationship between pecan ET using REEM and fc was investigated. The following conclusions were drawn from the study:

1. Pecan orchards in the Mesilla Valley covered an area of 9,758 ha (24,101 acres) as projected in the DOQQ mosaic. Seventy six percent of all the pecan orchards in

- the Valley were smaller than 4 ha (10 acres) but only constituted 19% of the total area;
2. Annual weighted ET means of 1,018 mm/year and 852 mm/year were determined for the orchards greater than 10 acres and less than 10 acres using REEM with Landsat-7 satellite data, respectively;
  3. Annual weighted ET means of 991 mm/year and 800 mm/year were determined for the orchards greater than 10 acres and less than 10 acres using REEM with ASTER satellite data, respectively;
  4. The values of  $f_c$  estimated with supervised classification of DOQQs for the orchards were within the range of measured values, with an absolute difference of 7% and average percent error of 14%;
  5. The NDVI was linearly correlated to  $f_c$  values on a field basis ( $R^2 = 0.71$ ); NDVI predicted  $f_c$  better when compared to SAVI and  $\theta_{SAVI}$ ;
  6. A single NDVI image from the middle of the growing season was related to REEM annual ET to develop a relationship for predicting annual ET for the pecan orchards as function of  $f_c$ .

### 7.3. Recommendations

In this study the relationship between ET and  $f_c$  (via NDVI) was derived using REEM and GIS vectors files. The accuracy of the REEM-estimated ET as well as the derived relationships to estimate ET as function of NDVI or  $f_c$  for pecan orchards needs to be verified by comparing it with a larger number of independent field measurements.



After comparing the REEM-ET estimates computed for the pecan orchards with values from the literature, it was concluded that the values estimated from the vectors (orchards) were lower than expected. This was partly due to the effects of the limited resolution of the TIR data which is used in ET calculations (ET maps), and to the lack of sufficient satellite images during the year. The impact and form in which the limited resolution of the TIR reflectance data affects the ET estimations made with surface energy balance (SEB) based models such as REEM needs to be studied thoroughly in future investigations. Supervised classification of DOQQs to determine  $f_c$  or pecan orchards produced reliable results when compared to a small number of field measurements carried out with two years of difference in a commercially oriented pecan farm. However, in order to verify this proposed method, a larger number of pecan orchards need to be measured at a time close to the time of acquisition of the satellite image or to the aerial spectral measurements. The measured orchards need to depict differences in tree size and age, tree densities, a wide range of  $f_c$  values, and must be under different agricultural management practices in order to encompass all possible conditions present in the Mesilla Valley.

This study focused only on pecans. However, by using the same analysis, regional water use or ET and its spatial variation could be determined for other crops in the Mesilla Valley. Spatial estimates of water use or ET at the orchard level could be used as a tool for decision-making in order to develop improved water management strategies within the river basin including better agricultural irrigation schemes and water conservation strategies.

## REFERENCES

- Abrams, M., Hook, S., and Ramachandran, B. (2002). *ASTER user handbook, ver. 2*. Pasadena, CA: California Institute of Technology, Jet Propulsion Laboratory. Retrieved October 18, 2007 from [http://asterweb.jpl.nasa.gov/content/03\\_data/04\\_Documents/aster\\_user\\_guide\\_v2.pdf](http://asterweb.jpl.nasa.gov/content/03_data/04_Documents/aster_user_guide_v2.pdf)
- Allen, R. G., Hendrickx, J. M. H., Toll, D., Anderson, M., Kustas, W., and Kleissl, J. (2008). From high overhead: ET measurement via remote sensing. *Southwest Hydrology*, 7, 30–33.
- Allen, R. G., Pereira, L. S., Raes, D., and Smith, M. (1998). *Crop evaporation: Guidelines for computing crop water requirements* (FAO Irrigation and Drainage Paper No. 56). Rome, Italy: Food and Agriculture Organization of the United Nations (FAO).
- Allen, R. G., Tasumi, M., Morse A., and Trezza, R. (2005a). A Landsat-based energy balance and evapotranspiration model in western U.S. water rights regulation and planning. *Irrigation and Drainage Systems*, 19, 251–268.
- Allen, R.G., Walter, I. A., Elliott, R. L., Howell T. A., Itenfisu, D., Jensen, M. E., et al. (Eds.). (2005b). *The American Society of Civil Engineers (ASCE) standardized reference evapotranspiration equation*. Reston, VA: American Society of Civil Engineers.
- Bastiaanssen, W. G. M. (1995). *Regionalization of surface flux densities and moisture indicators in composite terrain: A remote sensing approach under clear skies in Mediterranean climates*. Doctoral dissertation, Wageningen, the Netherlands: Landbouwniversiteit.
- Bastiaanssen, W. G. M. (1998). *Remote sensing in water resources management: The state of the art*. Colombo, Sri Lanka: International Water Management Institute.
- Bastiaanssen, W. G. M., Menenti, M., Feddes, R. A., and Holtslag, A. A. M. (1998a). A remote sensing surface energy balance algorithm for land (SEBAL), part 1: Formulation. *Journal of Hydrology*, 212–13, 198–212.
- Bastiaanssen, W. G. M., Noordman, E. J. M., Pelgrum, H., Davids, G., Thoreson B. P., and Allen R. G. (2005). SEBAL model with remotely sensed data to improve water-resources management under actual field conditions. *Journal of Irrigation and Drainage Engineering*, 131, 85–93.

- Bastiaanssen, W. G. M., Pelgrum, H., Wang, J., Ma, Y., Moreno, J.F., Roerink, G.J., et al. (1998b). A remote sensing surface energy balance algorithm for land (SEBAL), part 2: Validation. *Journal of Hydrology*, 212–13, 213–229.
- Bullock, H. E. and Neher, R. E. (1980). *Soil survey of Doña Ana County area, New Mexico*. Washington, DC: U.S. Government Printing Office.
- Carlson, T. N., and Ripley, D. (1997). On the relation between NDVI, fractional vegetation cover, and leaf area index. *Remote Sensing of Environment*, 62, 241–252.
- Choudhury, B. J., Ahmed, N. U., and Idso, S. B. (1994). Relations between evaporation coefficients and vegetation indices studied by model simulations. *Remote Sensing of Environment*, 50, 1–17.
- Clark, B., Soppe, R., Lal, D., Thoreson, B., Bastiaanssen, W., and Davids, G. (2007). Variability of crop coefficients in space and time - examples from California (pp. 481–499). In Clemmens, A. J. and Anderson, S. S. (Eds.) *Proceedings of the U.S. Committee on Irrigation and Drainage (USCID) Fourth International Conference on Irrigation and Drainage Sacramento, California, October 3-6, 2007*. Denver: U.S. Committee on Irrigation and Drainage.
- Dowdy, S., Wearden, S., and Chilko, D. (2004). *Statistics for Research*, third edition. Hoboken, New Jersey: John Wiley & Sons, Inc.
- Frías-Ramírez, J. E. (2002). *Physiological model of light interception and water use in pecan trees*. Unpublished doctoral dissertation. Las Cruces: New Mexico State University.
- Goodwin, I., Whitfield, D. M., and Connor, D. J. (2004). The relationship between peach tree transpiration and effective canopy cover. *Acta Horticulturae*, 664, 283–289.
- Groeneveld, D. P., Baugh, W. M., Sanderson, J. S., and Cooper, D. J. (2007). Annual groundwater evapotranspiration mapped from single satellite scenes. *Journal of Hydrology*, 344, 146–156.
- Hawley, J. W., and Kennedy, J. F. (2004). *Creation of a digital hydrogeologic framework model of the Mesilla Basin and Southern Jornada del Muerto Basin, New Mexico* (Technical Completion Report No. 332). Las Cruces: New Mexico State University, Water Resources Research Institute.

- Herrera, E. (2000). *Historical background of pecan planting in the Western region* (Guide H-626 PH 1-110). Retrieved November 11, 2007 from the New Mexico State University, College of Agriculture and Home Economics Web site: [http://www.cahe.nmsu.edu/pubs/\\_h/h-626.pdf](http://www.cahe.nmsu.edu/pubs/_h/h-626.pdf)
- Herrera, E. (2005). *Pecan varieties for New Mexico* (Guide H-639). Retrieved November 11, 2007 from the New Mexico State University, College of Agriculture and Home Economics Web site: [http://cahe.nmsu.edu/pubs/\\_h/h-639.pdf](http://cahe.nmsu.edu/pubs/_h/h-639.pdf)
- Huete, A. R. (1988). A soil adjusted vegetation index (SAVI). *Remote Sensing of Environment*, 25, 295–309.
- Huete, A. R., Jackson, R. D., and Post, D. F. (1985). Spectral response of a plant canopy with different soil backgrounds. *Remote Sensing of Environment*, 17, 37–53.
- Jiang, Z., Huete, A. R., Li, J., and Chen, Y. (2006). An analysis of angle-based with ratio-based vegetation indices. *IEEE Transactions on Geoscience and Remote Sensing*, 44, 2506–2513.
- Johnson, R. S. Ayars J., Trout, T., Mead, R. and Phene, C. (2000). Crop coefficients for mature peach trees are well correlated with midday canopy light interception. *Acta Horticulturae*, 537, 445–460.
- Johnson, R. S., Ayars, J., and Hsiao T. (2002). Modeling young peach tree evapotranspiration. *Acta Horticulturae*, 584, 107–113.
- King J. P., and Maitland J. (2003). *Water for river restoration: Potential for collaboration between agricultural and environmental water users in the Rio Grande Project area, report prepared for the Chihuahuan Desert Program and World Wildlife Fund (WWF)*. Retrieved December 13, 2007 from <http://cagesun.nmsu.edu/~jpkking/wwf/agH2O0603.pdf>
- Landsat Project Science Office (LPSO). (2007). *Landsat 7- Science data users handbook*. Retrieved October 10, 2007 from <http://landsathandbook.gsfc.nasa.gov/handbook.html>
- Liang, S., Fang, H., Hoogenboom, G., Teasdale, J., and Cavigelli, M. (2004). Estimation of crop yield at the regional scale from MODIS observations. *IGARSS 2001: Scanning the present and resolving the future: IEEE 2001 International Geoscience and Remote Sensing Symposium, 9-13 July 2001*,

- University of New South Wales, Sydney, Australia* (v.3, p.1625-1628). New York: Institute of Electrical Engineers.
- Malm, N. R. (2003). *Climate Guide: Las Cruces, 1892-2000*. (Research report No. 749). Retrieved May 20, 2008 from the New Mexico State University, College of Agriculture and Home Economics Web Site:  
[http://aces.nmsu.edu/pubs/research/weather\\_climate/rr749.pdf](http://aces.nmsu.edu/pubs/research/weather_climate/rr749.pdf)
- Manaster, J. (1994). *The pecan tree*. Austin: University of Texas Press.
- Markham, B. L. (1985). The Landsat sensor's spatial responses. *IEEE Transactions on Geoscience and Remote Sensing*, GE-23 (6), 864–875.
- Miyamoto, S. (1983). Consumptive water use of irrigated pecans. *Journal of the American Society for Horticultural Science*, 108, 676–681.
- New Mexico Office of the State Engineer (NM-OSE). (2000). *Lower Rio Grande Basin Hydrographic Survey report for Southern Mesilla Valley Section, Volume I: Water uses including irrigation near Las Cruces, Santo Tomas, Mesquite, San Miguel, La Mesa, Vado, Berino, Chamberino, Anthony, Strauss, Orange and Sunland Park part of Doña Ana Count*. Retrieved February 16, 2007 from the New Mexico Office of the State Engineer Web Site: <http://www.ose.state.nm.us/water-info/legal/LRG-Southern-Mesilla/smesvolumei.pdf>
- Or, D., and Groeneveld, D. P. (1994). Stochastic estimation of plant available soil water under fluctuating water table depths. *Journal of Hydrology*, 163, 43–64.
- Rahman, H., and Dedieu, G. (1994). SMAC: a simplified method for the atmospheric correction of satellite measurements in the solar spectrum. *International Journal of Remote Sensing*, 15, 123–143.
- Roerink, G. J., Bastiaanssen, W. G. M., Chambouleyron, J., and Menenti, M. (1997). Relating crop water consumption to irrigation water supply by remote sensing. *Water Resources Management*, 11, 445–465.
- Reveles, A. (2005). *Evapotranspiration of mature pecan trees*. Unpublished Master's thesis. Las Cruces: New Mexico State University.
- Samani, Z., Bawazir, A. S., Bleiweiss, M., Skaggs, Longworth, J., Tran, V., and Piñón, A. (2009). Using remote sensing to evaluate the spatial variability of evapotranspiration and crop coefficient in the lower Rio Grande Valley, New Mexico. *Irrigation Science*, 28, 93–100.

- Samani, Z., Bawazir, A. S., Bleiweiss, M. P., and Skaggs, R. K. (2007a). Estimating pecan water use through remote sensing in the Lower Rio Grande (pp. 253–260). In Clemmens, A. J. and Anderson, S. S. (Eds.). *Proceedings of the USCID Fourth International Conference on Irrigation and Drainage, Sacramento, California, October 3-6, 2007*. Denver: U.S. Committee on Irrigation and Drainage.
- Samani, Z., Bawazir, A. S., Skaggs, R. K., Bleiweiss, M. P., Piñón, A., and Tran, V. (2007b). Water use by agricultural crops and riparian vegetation: An application of remote sensing technology. *Journal of Contemporary Water Research & Education*, 137, 8–13.
- Sammis, T. W., Mexal, J. G., and Miller, D. (2004). Evapotranspiration of flood irrigated pecans. *Agricultural Water Management*, 69, 179–190.
- Skaggs, R. K., and Samani, Z. (2005). Farm size, irrigation practices, and on-farm irrigation efficiency. *Irrigation and Drainage*, 54, 43–57.
- Sparks, D. (2005). Adaptability of pecan as a species. *HortScience*, 40, 1175–1189.
- Steinberg, S. L., McFarland, M. J. and Worthington, J. W. (1990). Comparison of trunk and branch sap flow with canopy transpiration in pecan. *Journal of Experimental Botany*, 41, 653–659.
- Tasumi, M., Allen, R. G., Trezza, R., and Wright J. L. (2005). Satellite-based energy balance to assess within-population variance of crop coefficient curves. *Journal of Irrigation and Drainage Engineering*, 131, 94–109.
- Trout, T. J., and Johnson, L. F. (2007). Estimating crop water use from remotely sensed NDVI, crop models and reference ET (pp. 275–285). In Clemmens, A. J. and Anderson, S. S. (Eds.). *Proceedings of the USCID Fourth International Conference on Irrigation and Drainage, Sacramento, California, October 3-6, 2007*. Denver: U.S. Committee on Irrigation and Drainage.
- Tucker, C. J. (1979). Red and photographic infrared linear combinations for monitoring vegetation. *Remote Sensing of Environment*, 8, 127–150.
- U.S. Bureau of the Census. (1961). *1959 Census of Agriculture. Vol. I. Counties, Part 42: New Mexico* (pp.158–159). Washington, DC: U.S. Government Printing Office.

- U.S. Bureau of the Census. (1967). *1964 Census of Agriculture. Statistics for the state and counties, Volume I, Part 42: New Mexico* (pp. 288–289). Washington, DC: U.S. Government Printing Office.
- U.S. Bureau of the Census. (1977). *1974 Census of Agriculture. Volume I, Part 31: New Mexico state and county data* (p. III-8). Washington, DC: U.S. Government Printing Office.
- U.S. Bureau of the Census. (1981). *1978 Census of Agriculture. Volume I, Part 31: New Mexico state and county data* (pp. 148–149). Washington, DC: U.S. Government Printing Office.
- U.S. Bureau of the Census. (1984). *1982 Census of Agriculture. Volume I. Geographic area series, Part 31: New Mexico state and county data* (p. 247). Washington, DC: U.S. Government Printing Office.
- U.S. Bureau of the Census. (1989). *1987 Census of Agriculture. Volume I. Geographic area series, Part 31: New Mexico state and county data* (p. 271). Washington, DC: U.S. Government Printing Office.
- U.S. National Agricultural Statistics Service (NASS). (2004). *Agricultural statistics 2004*. Retrieved November 23, 2007 from the NAAS publications Web site: [http://www.usda.gov/nass/pubs/agr04/04\\_ch5.pdf](http://www.usda.gov/nass/pubs/agr04/04_ch5.pdf).
- U.S. National Agricultural Statistics Service (NASS). (2007). *2002, 1997 and 1992 Census of Agriculture, New Mexico state and county data. Volume 1: geographic area series*. Retrieved August 7, 2007 from the U.S. Department of Agriculture: *The Census of Agriculture* Web site: <http://www.agcensus.usda.gov/>
- U.S. National Agricultural Statistics Service (NASS). (2010). *2007 Census of Agriculture, New Mexico state and county data. Volume 1, Chapter 2: County Level Data*. Retrieved November 23, 2010 from the U.S. Department of Agriculture: *The Census of Agriculture* Web site: <http://www.agcensus.usda.gov/publications/2007/index.asp>.
- U.S. New Mexico Agricultural Statistics (NMAS). (2002). *Annual statistical bulletin. Pecans: orchards, acres and production by county*. Retrieved February 27, 2008 from <http://www.nass.usda.gov/nm/nmbulletin/62-02.pdf>
- U.S. New Mexico Agricultural Statistics (NMAS). (2004). *Annual statistical bulletin. Pecans: orchards, acres and production by county*. Retrieved November 15, 2007 from <http://www.nass.usda.gov/nm/nmbulletin/62-04.pdf>

U.S. New Mexico Agricultural Statistics (NMAS). (2006). *Annual statistical bulletin. Pecans: orchards, acres and production by county*. Retrieved February 27, 2008 from [http://www.nass.usda.gov/Statistics\\_by\\_State/New\\_Mexico/Publications/Annual\\_Statistical\\_Bulletin/2006/61\\_06.pdf](http://www.nass.usda.gov/Statistics_by_State/New_Mexico/Publications/Annual_Statistical_Bulletin/2006/61_06.pdf)

Weeden, A. C., and Maddock, T. III. (1999). *Simulation of groundwater flow in the Rincon Valley area and Mesilla Basin, New Mexico, and Texas* (p. 187). Tucson: University of Arizona Research Laboratory for Riparian Studies and Department of Hydrology and Water Resources.